Boise State University
ScholarWorks

Geosciences Faculty Publications and Presentations | Department of Geosciences

9-1-2014

Postglacial Early Permian (Late Sakmarian– Early Artinskian) Shallow-Marine Carbonate Deposition Along a 2000 km Transect from Timor to West Australia

Vladimir I. Davydov
Boise State University

NOTICE: this is the author's version of a work that was accepted for publication in *Palaeogeography, Palaeoclimatology, Palaeoecology*. Changes resulting from the publishing process, such as peer review, editing, corrections, structural formatting, and other quality control mechanisms may not be reflected in this document. Changes may have been made to this work since it was submitted for publication. A definitive version was subsequently published in *Palaeogeography, Palaeoclimatology, Palaeoecology*, (In Press). doi: 10.1016/j.palaeo.2014.05.009

This is an author-produced, peer-reviewed version of this article. The final, definitive version of this document can be found online at *Palaeogeography, Palaeoclimatology, Palaeoecology*, published by Elsevier. Copyright restrictions may apply. doi: 10.1016/j.palaeo.2014.05.009

Postglacial Early Permian (late Sakmarian– early Artinskian) shallow-marine carbonate deposition along a 2000 km transect from Timor to west Australia

David W. Haig[a], Eujay McCartain[b], Arthur J. Mory[bc], Gilsel Borges[d], Vladimir I. Davydov[e], Matthew Dixon[bj], Andrej Ernst[f], Stefan Groflin[g], Eckart Håkansson[a], Myra Keep[b], Zelia Dos Santos[bi], G.R. Shi[h], Jacinto Soares[c]

Corresponding author: D. W. Haig email: david.haig@uwa.edu.au

[a]*Centre for Petroleum Geoscience and CO_2 Sequestration, School of Earth and Environment (M004), The University of Western Australia, 35 Stirling Highway, Crawley 6009, Australia*

[b]*School of Earth and Enivronment (M004), The University of Western Australia, 35 Stirling Highway, Crawley WA 6009, Australia*

[c]*Geological Survey of Western Australia, Department of Mines and Petroleum, 100 Plain St., East Perth, WA 6004, Australia*

[d]*Eni Timor-Leste Ltd., P.O. Box 52, Dili, Timor-Leste*

[e]*Permian Research Institute, Boise State University, 1910 University Drive, Boise, ID, USA*

[f]*Institut für Geologie, Universität Hamburg, Bundesstrasse 55, D-20146 Hamburg, Germany*

[g]*Earth, Environmental and Biological Sciences, Queensland University of Technology, Brisbane Queensland 4001, Australia*

[h] *School of Life and Environmental Sciences, Deakin University, 221 Burwood Highway, Burwood, Victoria 3125, Australia*

[i] *Present address: Timor Gap, E.P. Level 3, Timor Plaza, Suit 301-314 Rua Presidente Nicolao, Comoro Dili Timor-Leste*

[j]*Present address: Shell Development (Australia) Pty Ltd, GPO Box A47 CDC, Perth WA 6837, Australia*

This is an author-produced, peer-reviewed version of this article. The final, definitive version of this document can be found online at *Palaeogeography, Palaeoclimatology, Palaeoecology*, published by Elsevier. Copyright restrictions may apply. doi: 10.1016/j.palaeo.2014.05.009

ABSTRACT

Late Sakmarian to early Artinskian (Early Permian) carbonate deposition was widespread in the marine intracratonic rift basins that extended into the interior of Eastern Gondwana from Timor in the north to the northern Perth Basin in the south. These basins spanned about 20° of paleolatitude (approximately 35°S to 55°S). This study describes the type section of the Maubisse Limestone in Timor-Leste, and compares this unit with carbonate sections in the Canning Basin (Nura Nura Member of the Poole Sandstone), the Southern Carnarvon Basin (Callytharra Formation) and the northern Perth Basin (Fossil Cliff Member of the Holmwood Shale). The carbonate units have no glacial influence and formed part of a major depositional cycle that, in the southern basins, overlies glacially influenced strata and lies a short distance below mudstone containing marine fossils and scattered dropstones (perhaps indicative of sea ice). In the south marine conditions became more restricted and were replaced by coal measures at the top of the depositional sequence. In the north, the carbonate deposits are possibly bryozoan–crinoidal mounds; whereas in the southern basins they form thin laterally continuous relatively thin beds, deposited on a very low-gradient seafloor, at the tops of shale–limestone parasequences that thicken upward in parasequence sets. All marine deposition within the sequence took place under very shallow (inner neritic) conditions, and the limestones have similar grain composition. Bryozoan and crinoidal debris dominate the grain assemblages and brachiopod shell fragments, foraminifera and ostracod valves are usually common. *Tubiphytes* ranged as far south as the Southern Carnarvon Basin, albeit rarely, but is more common to the north. Gastropod and bivalve shell debris, echinoid spines, solitary rugose corals and trilobite carapace elements are rare. The uniformity of the grain assemblage and the lack of tropical elements such as larger fusulinid foraminifera, colonial

This is an author-produced, peer-reviewed version of this article. The final, definitive version of this document can be found online at *Palaeogeography, Palaeoclimatology, Palaeoecology*, published by Elsevier. Copyright restrictions may apply. doi: 10.1016/j.palaeo.2014.05.009

corals or dasycladacean algae indicate temperate marine conditions with only a small increase in temperature to the north.

The depositional cycle containing the studied carbonate deposits represents a warmer phase than the preceding glacially influenced Asselian to early Sakmarian interval and the subsequent cool phase of the "mid" Artinskian that is followed by significant warming during the late Artinskian–early Kungurian. The timing of cooler and warmer intervals in the west Australian basins seems out-of-phase with the eastern Australian succession, but this may be a problem of chronostratigraphic miscorrelation due to endemic faunas and palynofloras.

Keywords

Early Permian

Sakmarian–Artinskian

Carbonate

Intracratonic

Eastern Gondwana

N–S temperature gradient

This is an author-produced, peer-reviewed version of this article. The final, definitive version of this document can be found online at *Palaeogeography, Palaeoclimatology, Palaeoecology*, published by Elsevier. Copyright restrictions may apply. doi: 10.1016/j.palaeo.2014.05.009

1. Introduction

Teichert (1939) proposed a connection between the Permian of Timor and coeval deposits in west Australian basins and suggested continuity between his “Westralian Geosyncline”, including what are now broadly termed the Canning, Southern Carnarvon and Perth Basins (Fig. 1), and the "Timor–East Celebes Geosyncline" now known as the Outer Banda Arc (Audley-Charles, 1968). Most early stratigraphic work on Timor suggested that the Permian limestones and associated volcanic units were tectonically allochthonous (e.g. Brouwer, 1942; Gageonnet and Lemoine, 1958; Audley-Charles, 1968; Carter et al., 1976; Brunnschweiler, 1978). By contrast, paleomagnetic studies (Chamalaun, 1977; Wensink and Hartosukohardjo, 1990) as well as a re-evaluation of Permian faunas and floras (Archbold, et al., 1982; Webster, 1998; Charlton et al., 2002; McCartain et al., 2006) and a better understanding of the tectonic makeup of present-day South East Asia (Hall and Sevastjanova, 2012) have contributed to now almost general acceptance that the Timor Permian was deposited in a northern Gondwanan basin that was closely linked to basins along the present west Australian margin. These basins formed a broad belt, informally designated the East Gondwana interior rift system (Fig. 1; previously termed the "Western Australian Trough" by Wopfner, 1999), along which continental breakup took place during the Jurassic and Early Cretaceous to form the present Indian Ocean (Audley-Charles, 1983, 1984, 1988; Veevers, 1988; Harrowfield et al., 2005; Heine and Müller, 2005; Ali et al., 2013).

Earliest Permian deposition in the East Gondwana interior rift system included glacially derived sediment, at least in the west Australian basins (Eyles and Eyles, 2000; Eyles et al. 2003; Eyles et al., 2006; Gorter et al., 2008; Mory et al., 2008). By the late Sakmarian and throughout the early Artinskian, there was no glacial influence throughout the rift system in the studied region and seas flooded as far south as the northern Perth Basin (see

This is an author-produced, peer-reviewed version of this article. The final, definitive version of this document can be found online at *Palaeogeography, Palaeoclimatology, Palaeoecology*, published by Elsevier. Copyright restrictions may apply. doi: 10.1016/j.palaeo.2014.05.009

Sections 3–7, herein). At this time, carbonate deposits were widespread in Timor (Maubisse Formation; Charlton et al., 2002) whereas fine-grained siliciclastic facies including minor carbonates dominated west Australian onshore basins (Veevers and Wells, 1961; Playford et al., 1976; Hocking et al., 1987; Mory, 1991). The Lower Permian is very poorly known in offshore basins in Western Australia because it is deeply buried under thick Mesozoic successions. This paper sets out to document the primary composition of the limestone facies within the first post-glacial depositional sequence of the Lower Permian along the East Gondwana interior rift system, from Timor in the north to the northern Perth Basin in the south. Very little has been published on the composition of the original sediment forming the late Sakmarian–early Artinskian limestone units in these basins. Dixon and Haig (2004) presented a detailed account of the biogenic components of shale and interbedded limestone from the type section of the Callytharra Formation (Fig. 2) in the southern part of the Southern Carnarvon Basin (locality 7 of Fig. 1). Frank et al. (2012) provided a more general account of biogenic components from thin sections of selected levels within the same formation from three boreholes located near the margins of this basin.

Our study provides the first detailed description of the Maubisse Formation at its type locality in Timor Leste (locality 1, Fig. 1), determines the composition and age of the limestone, and compares its composition with that of coeval limestones in west Australian basins further south in the East Gondwana rift system (localities 2–8, Figs. 1, 2). This 2000 km transect brings new insights into the nature of the late Sakmarian–early Artinskian sea that flooded the interior of eastern Gondwana following melting of continental ice sheets in this region and of the biota that produced extensive carbonate deposits. It also provides a greater appreciation of intracratonic climate gradients through mid- to high latitudes after one of the major ice ages in the Earth's history. The late Sakmarian–early Artinskian interval including the carbonate deposition documented here is apparently coeval with Glaciation P2 in the

This is an author-produced, peer-reviewed version of this article. The final, definitive version of this document can be found online at *Palaeogeography, Palaeoclimatology, Palaeoecology*, published by Elsevier. Copyright restrictions may apply. doi: 10.1016/j.palaeo.2014.05.009

eastern Australian Permian basins (Fielding et al., 2008a,b,c). Therefore a major conundrum exists as to why the west Australian phases of warming and cooling during the Early Permian seem to be out-of-phase with those reported from eastern Australia.

2. Material and Methods

A type section was selected at Audley-Charles' (1968) type locality of the Maubisse Formation (sections 3, 4) and measured using an Abney Level and Jacob Staff, systematically sampled, and where accessible logged using a gamma-ray scintillometer at 0.25 m intervals. In Western Australian basins, the following type sections were measured and sampled: the Nura Nura Limestone in the Canning Basin; Callytharra Formation and Jimba Jimba Calcarenite in the Southern Carnarvon Basin; and Fossil Cliff Member of Holmwood Shale in the Northern Perth Basin. In the Southern Carnarvon Basin additional outcrop sections were measured through the Callytharra Formation at Dead Man's Gully and along the Lyndon River (see Appendix A; Supplementary Material), and a continuous core of the Nura Nura Limestone from the Canning Basin was studied. Although equivalent carbonate units are also known from the Bonaparte Basin, outcrops are ferruginized and no core from this basin is available.

Limestone samples were slabbed and acetate peels made by etching the slabbed surface in 2 % hydrochloric acid for 3–4 minutes, flooding the dried etched surface with acetone, and placing a sheet of acetate paper on the surface before the acetone evaporated. Under transmitted light, acetate peels show the fine microstructure of biogenic carbonate grains, allowing identification of grains, matrix and cement. Because a large surface may be examined on the peel, a better appreciation of the composition of the limestone can be obtained from such peels than from smaller thin sections because larger surfaces can be

This is an author-produced, peer-reviewed version of this article. The final, definitive version of this document can be found online at *Palaeogeography, Palaeoclimatology, Palaeoecology*, published by Elsevier. Copyright restrictions may apply. doi: 10.1016/j.palaeo.2014.05.009

examined, and at considerably less cost and time. Thin sections were made of some of the samples from the Canning and Southern Carnarvon Basins. Continuous acetate peels were made of core from the Nura Nura Member, Canning Basin. The relative abundance of biogenic grain types was determined by DWH based on visual estimation (using consistent abundant, common and rare categories) from peels and thin sections using a transmitted light microscope. Samples from limestone beds at 10 m, 12 m, 15 m, 55 m, 68 m, 84 m, 90 m, 92 m, 110 m, 112 m, 122 m, 155 m, 177 m, and 180 m in the section were processed for conodonts by digestion in ~7% acetic acid. However, none were found from 10 kg of rock.

Outcrop gamma was attempted at the type section of the Maubisse Formation using a small scintillometer with measurements taken every 25 cm (apart from over covered intervals) to attempt to differentiate subtle cyclicity in the limestone. Only total gamma was measured incorporating emissions from K, U and Th.

It is intended that the material we have acquired will form the bases for taxonomic studies of certain fossil groups (especially the bryozoans and foraminifera) and may prompt more detailed analysis of facies and limestone diagenesis. All material is housed in the collections at the University of Western Australia (Earth Science Museum) and the Geological Survey of Western Australia. Duplicates of samples from Timor are in the collections of the Institute of Petroleum and Geology of Timor-Leste.

3. Overview of the Lower Permian stratigraphy of Timor

Although Permian studies of Timor have yielded a vast inventory of marine invertebrate fossils, its internal stratigraphy is poorly understood because of great structural complexity (Webster, 1998; Charlton et al., 2002; Meijer, et al., 2009). In West Timor, detailed mapping in 1937 by geologists from the University of Amsterdam grouped the

This is an author-produced, peer-reviewed version of this article. The final, definitive version of this document can be found online at *Palaeogeography, Palaeoclimatology, Palaeoecology*, published by Elsevier. Copyright restrictions may apply. doi: 10.1016/j.palaeo.2014.05.009

Permian to Mesozoic strata into two tectonostratigraphic divisions with "flysch facies" placed in the Kekneno series and carbonate and volcanic facies in the Sonnebait series (summarized by Brouwer, 1942). In eastern Timor, Gageonnet and Lemoine (1958) defined the “Série de Cribas” for a Permian mainly siliciclastic succession (equivalent to the Kekneno series) in the Cribas Anticline; and the Permian “Série de Maubisse” comprising a lower unit of metamorphic rocks (> 1000 m thick) and an upper unit, equivalent to the Sonnebait series, of shallow-marine carbonates (200–400 m thick) and volcanics (> 500 m thick). Although Audley-Charles (1968) designated the upper unit as the Maubisse Formation and selected a type locality in limestone cliffs southwest of the town of Maubisse (Fig. 3), he did not provide a stratigraphic log of the type section and his discussion of fossil assemblages and age appears to be derived from unspecified localities throughout Timor-Leste. Subsequent to the initial definition of the Maubisse Formation as a Permian unit, Triassic and younger rocks have also been assigned to this unit (e.g. Villeneuve et al., 2005). A detailed evaluation of the internal stratigraphy of the Maubisse Formation has been attempted only in eastern West Timor where “units” of apparent Sakmarian–Artinskian age have been described (unpublished study of Barkham summarized in Archbold and Barkham, 1989; Charlton et al., 2002; and Riding and Barkham, 1999).

Many fossil assemblages reported from the Timor Permian contain stratigraphically mixed material (Webster, 1998; Charlton et al., 2002). Only a few Lower Permian localities, well positioned in terms of local lithostratigraphy, have been dated by conodonts, fusulinids, or ammonoids. These localities indicate, albeit tentatively, an uppermost Pennsylvanian to lowest Asselian limestone succession containing reef-buildups at the base associated with volcanics (Daydov et al., 2013). This is followed, at least in the upper Asselian and Sakmarian, by a dominantly sand–shale–volcaniclastic succession with some interbedded limestone units (ammonoid assemblages discussed by H.G. Owen in Charlton et al., 2002,

This is an author-produced, peer-reviewed version of this article. The final, definitive version of this document can be found online at *Palaeogeography, Palaeoclimatology, Palaeoecology*, published by Elsevier. Copyright restrictions may apply. doi: 10.1016/j.palaeo.2014.05.009

based on collections made by P.R. Bird; conodont assemblages from the southwest Mutis region discussed by van den Boogaard, 1987; unpublished conodont occurrences of E. McCartain). A major change is suggested in the upper Sakmarian–lower Artinskian where thick limestone successions are recorded on the basis of limited conodont and brachiopod data (Archbold and Barkham, 1989; Nicoll and Metcalfe, 1998, based on collections made by S.T. Barkham; present study). These deposits probably represent the thickest carbonate accumulations in the Timor Permian. Isolated limestones containing the larger fusulinid *Monodiexodina wanneri*, either in monospecific assemblages or associated with *Schwagerina brouweri* may belong within the late Artinskian or Kungurian (Schubert, 1915; Thompson, 1949; unpublished fusulinid occurrences determined by V. Davydov based on collections made by D. Haig). Based on Leonova's (2011) assessment of the ammonoids, the Kungurian also includes the Bitauni beds (mainly red mudstone–marl) of West Timor (Charlton et al., 2002) from which Van den Boogaard (1987) described conodonts. Because of great structural complexity (Hamilton, 1979) and inadequate detailed mapping, a geological map showing the distribution of Permian stratigraphic units cannot be compiled at present and a detailed stratigraphic correlation chart is premature.

4. Maubisse Limestone Type Area

4.1. Type area

Audley-Charles (1968) selected a prominent limestone ridge (Fig. 4) to the southwest of Maubisse as the type locality of the "Maubisse Formation". The ridge, which includes Fatu Rabi (or Mount Hatorobi), has a steep scarp on the south side and a more gentle dip slope (about 40°) to the north. It extends from 8.851393°S, 125.578010°E along strike, in places

This is an author-produced, peer-reviewed version of this article. The final, definitive version of this document can be found online at *Palaeogeography, Palaeoclimatology, Palaeoecology*, published by Elsevier. Copyright restrictions may apply. doi: 10.1016/j.palaeo.2014.05.009

displaced by high-angle faulting, as high cliffs to 8.854412°S, 125.562002°E and then as a lower ridge to about 8.853837°S, 125.554267°E. The total outcrop length along strike is ~2.6 km (Fig. 5). High-angle faults obliquely cut the ridge and displace the crests by up to 500 m. A strike-parallel high-angle fault repeats the stratigraphic succession immediately south of the main ridge in less well-exposed outcrop.

The cliffs at the type locality are composed of a coherent limestone succession about 180 m thick and not overturned (see 3.2). Audley-Charles (1968) also placed at least 500 m of basic volcanic rocks outcropping on the slopes of Mt Ramelau (Fig. 4A) as the upper part of the "Maubisse Formation". This succession is not present at the type locality and a series of major faults, oblique to the limestone ridge, separate the limestone succession from rock units on the hills that lead to Mt Ramelau (Figs 4A, 5). There is no evidence to associate the volcanic succession on Mt Ramelau with a conformable stratigraphic unit above the limestone succession. As part of the refinement of lithostratigraphy in Timor, it is proposed to rename Audley-Charles's "Maubisse Formation" as the "Maubisse Limestone" with the section we measured here on the limestone ridge as type section (see 3.2).

The outcrop pattern of the Maubisse Limestone along the ridge (Fig. 5) indicates that the thickness of the formation may decrease towards the west and that the carbonate facies may be lenticular. Large limestone lenses are present elsewhere in Timor-Leste (e.g. the uppermost Gzhelian bioherm described by Davydov et al., 2013, from Kulau); and we found three lenticular Permian limestones on a prominent ridge about 3 km north–northwest of the type section of the Maubisse Limestone.

4.2. Type section

This is an author-produced, peer-reviewed version of this article. The final, definitive version of this document can be found online at *Palaeogeography, Palaeoclimatology, Palaeoecology*, published by Elsevier. Copyright restrictions may apply. doi: 10.1016/j.palaeo.2014.05.009

The ridge is composed of a succession of massive to thick-bedded limestone. The western end of the steep ridge near the village of Maunlai is the most accessible place to examine the entire stratigraphic section (Fig. 4). Here detailed measurement of a continuous 95 m section through part of the limestone succession is possible on a moderately steep slope adjacent to a fault-truncated section between 8.85486°S, 125.56278°E and 8.85422°S, 125.56243°E. Immediately above, the cliff is too steep for detailed logging, and outcrop is discontinuous at the top of the succession on the ridge crest. Outcrop of the lower part of the succession, below the base of the measured section at 8.85486°S, 125.56278°E, also is discontinuous. Therefore thicknesses were estimated, from a stratigraphic cross-section, in the lower and upper parts of the succession (Fig. 6).

The limestone at the type locality is estimated to be 180 m thick, whereas Audley-Charles (1968, p. 43, 44) cited 400 m; Crostella and Powell (1975) 150 m; and Charlton et al. (2002, p. 725) 60 m based on an unpublished 1993 study by D.C. Hunter. The interval between 30 m and 62 m consists of massive limestone. Above this level, the succession is thick bedded with possible friable lithologies (perhaps mudstone) in covered intervals at 82–84 m, 118–123 m, 125–128 m and at several higher levels that could not be logged accurately. In the upper part of the section, tabular thick bedding can be traced along the Maunlai ridge to the east of the type section. Geopetal structures in closed brachiopod shells in the upper part of the succession indicate that the section has not been overturned. The limestone succession overlies, with apparent conformity, an un-named volcaniclastic–siliciclastic succession that includes weathered basalt. These older rocks outcrop very poorly, but include an upper volcaniclastic unit (containing some basalt) that is about 30 m thick above grey shale.

The northern dip slope of the main ridge marks the top of the limestone succession. The overlying friable succession has largely been removed by erosion (Fig. 4A), but small patches of weathered mudstone and some thin sandstone interbeds belonging to an un-named

This is an author-produced, peer-reviewed version of this article. The final, definitive version of this document can be found online at *Palaeogeography, Palaeoclimatology, Palaeoecology*, published by Elsevier. Copyright restrictions may apply. doi: 10.1016/j.palaeo.2014.05.009

formation are preserved above the limestone and a conformable contact is exposed at 08.85255° S, 125.56293° E.

Outcrop gamma run over the measured section reveals a series of 5–15 m thick cycles up to about 80 m in the section, presumably shoaling upward based on upward decreasing counts: discounting input from U and Th, cleaner intervals contain less K indicative of less clay and likely higher-energy facies. Above 80 m there is a moderate increase in the gamma count possibly suggestive of lower energy facies, although there is also some indication of shoaling upwards cycles, especially around 83–89 m and 107–113 m. The overall gamma profile can be interpreted as a series of progradational cycles up to about 80 m followed by retrogradational cycles, albeit irregular (Fig. 6). Because of difficulties in observing rock details on the cliff face, cyclicity was not apparent from visual inspection of the outcrop.

4.3. Limestone composition

Limestone beds within the section are entirely bioclastic and mainly packstone (Appendix A, Supplementary Materials; Fig. 6) but with variable grain density. In many beds the carbonate matrix is partially recrystallized. In a few beds, particularly between 110 m and 130 m, thick radaxial isopachous cement surrounding bryozoans is present. Dolomite is common between 30 m and 50 m, probably associated with the oblique fault that exposes this part of the section. The limestone between 30 m and 47 m is brecciated, likely also due to the fault. Although in many samples grains are bored resulting in fine branching tubes penetrating the periphery of skeletons perhaps formed by endolithic cyanobacteria (Flügel, 2004), there are no micritic envelops or cyanobacterial encrustations around grains. Ooids and peloids are absent.

This is an author-produced, peer-reviewed version of this article. The final, definitive version of this document can be found online at *Palaeogeography, Palaeoclimatology, Palaeoecology*, published by Elsevier. Copyright restrictions may apply. doi: 10.1016/j.palaeo.2014.05.009

Bryozoan fragments and crinoid debris dominate the grain assemblage (Fig. 6). *Tubiphytes* (Fig. 7A–C; following the terminology of Senowbari-Daryan, 2013) are absent in the basal part of the section, but are common above 55 m. Brachiopod debris, foraminifera, ostracod valves, gastropods, echinoid spines, trilobite carapace debris, fragments of bivalve shells with prismatic microstructure, and solitary rugose corals are rare components. Of these grain types, the bryozoans and foraminifera have the greatest potential for future taxonomic discrimination at genus and possibly species level.

The bryozoans are present as slightly abraded sand-sized grains to larger, non-abraded fragments of colonies. A very low diversity bryozoan fauna from 30–50 m is composed almost exclusively by fragments of delicate colonies of the Order Fenestrata, dominated by *Spinofenestella* (Fig. 8K). Above, a higher diversity bryozoan assemblage, peaking around 60 m and 120 m, is composed mainly of fragile colonies with fragments of more robust colonies largely restricted to the two maxima intervals. The fauna is mainly delicate and robust Fenestrata with common arborescent Cryptostomata as well as minor arborescent Trepostomata and Cystoporata. Encrusting taxa are generally rare.

The foraminifera include calcivertellines (Order Miliolida; Fig. 9A1–A3) as the most common types, with rare simple Fusulinida including endothyraceans (Fig. 9D1), tetrataxaceans (Fig. 9E1–E2), lasiodiscids (Fig. 9F1–F2) and pseudoammodiscids (Fig. 9G1) but not in all samples. No larger Fusulinida were found. Specimens of the Order Lagenida (interpreted as in Groves et al., 2004) are the least abundant of the foraminifera and are recognized in only 7 of the 96 samples from the section.

4.4 Age

This is an author-produced, peer-reviewed version of this article. The final, definitive version of this document can be found online at *Palaeogeography, Palaeoclimatology, Palaeoecology*, published by Elsevier. Copyright restrictions may apply. doi: 10.1016/j.palaeo.2014.05.009

Although no conodonts were recovered from the type section, a sample from 320 m further west along the limestone ridge (Fig. 10A) yielded a Pa element fragment (Fig. 10B,C) identified as probably *Vjalovognathus australis* Nicoll and Metcalfe. Although endemic to southern cool-water successions, the species indicates a late Sakmarian–Artinskian age based on west Australian successions (Nicoll and Metcalfe, 1998), and has been identified previously from limestone of this age in West Timor (as *Vjalovognathus shindyensis* by van den Boogaard, 1987, according to Nicoll and Metcalfe, 1998, p. 454).

No ammonoids were found in the limestone. Macrofossils extracted as free specimens from the limestone section include only poorly preserved brachiopods that remain to be identified. A small collection of slightly better preserved brachiopods from scree at 8.85389°S, 125.56601°E immediately in front of the steep scarp of Maunlai ridge yielded incomplete specimens (lacking internal details) of probable *Cimmeriella foordi* (Etheridge). The species is known from the lower Callytharra Formation in the Southern Carnarvon Basin and the Fossil Cliff Member in the northern Perth Basin (see sections 6 and 7). Globally, confirmed occurrences of *Cimmeriella* are within the Sakmarian to lower Artinskian (Archbold and Hogeboom, 2000) and have a distinctive bi-temperate distribution (defined as in Shi et al., 1995), in that its species appear to have been restricted to temperate middle-latitude marine basins of both hemispheres. The genus is missing from true cold-water polar environments such as the eastern Australian basins.

5. Canning Basin

5.1 Overview of Sakmarian–Artinskian sequence

This is an author-produced, peer-reviewed version of this article. The final, definitive version of this document can be found online at *Palaeogeography, Palaeoclimatology, Palaeoecology*, published by Elsevier. Copyright restrictions may apply. doi: 10.1016/j.palaeo.2014.05.009

Uppermost Carboniferous and Lower Permian deposits of the Canning Basin accumulated in a large interior rift along an axis trending southeast from the main north–south interior-rift system (Fig. 1). The Poole Sandstone forms an upper Sakmarian–lower Artinskian depositional sequence of shallow-marine to deltaic facies in the Canning Basin (Fig. 2; Guppy et al., 1958; Playford et al., 1975; Mory, 2010). At the base of the Poole Sandstone, a 10–15 m thick succession of fossiliferous calcareous quartz sandstone and rare limestone interbedded with friable fine-grained sandstone forms the Nura Nura Member (Guppy et al., 1958; Playford et al., 1975; Crowe and Towner, 1976; Mory, 2010). The underlying Grant Group is composed of a thick sandstone-dominated succession that is interpreted as either glacially influenced (Redfern and Millward, 1994) or as resulting from phases of local tectonic subsidence with some reworking of glacial sediment (Eyles and Eyles, 2000), although these interpretations are not mutually exclusive (Mory et al., 2008). The top of the Poole Sandstone is terminated by marine-flooding that resulted in deposition of the mud-dominated facies of the Noonkanbah Formation that is, at least in its upper part, Kungurian in age (Nicoll and Metcalfe, 1998). No glacial influence has been recorded within the sequence.

5.2 Composition of limestone in Nura Nura Member

Limestone samples from two localities have been examined: the type area of the member in the inner Canning Basin (locality 3 on Fig 1; Appendix A, Supplementary Material); and the upper part of core 1 from 872.0 m to 877.06 m in the Perindi 1 exploratory well (locality 2 on Fig. 1; Appendix A, Supplementary Material) in the outer Canning Basin. The well lies closer to the main axis of the interior-rift system than the type area and contains

This is an author-produced, peer-reviewed version of this article. The final, definitive version of this document can be found online at *Palaeogeography, Palaeoclimatology, Palaeoecology*, published by Elsevier. Copyright restrictions may apply. doi: 10.1016/j.palaeo.2014.05.009

a thicker continuous limestone succession than in the type area, probably reflecting an increasing marine influence to the northwest in the basin.

Exposure of the Nura Nura Member in the type area is limited and discontinuous. Indurated beds, which are interbedded with friable units that are not exposed, include mainly calcareous quartz sandstone that contains rare to abundant brachiopod debris. Other biogenic grains in these coarse-grained sandstone beds are rare and include foraminifera, bryozoan fragments, and ostracod valves. The wackestone–packstone within the member contains a more diverse assemblage including abundant brachiopod debris, common ostracod valves, rare foraminifera, rare bryozoan fragments and encrustations on brachiopod valves, and very rare gastropods, bivalve shell fragments with prismatic microstructure and crinoid(?) plates. The brachiopod shells have been affected by minor cyanobacterial boring, but micritic envelopes are not developed around any grains. The foraminifera are mainly hemigordiopsids (Fig. 9B1–B3) with very rare calcivertellines and lagenids (probably *Protonodosaria*). The bryozoans include large free fragments and encrusting colonies of robust Cystoporata and Fenestrata.

Core 1 from Perindi 1 includes a limestone section between 872.0 m to 877.06 m that lies at the base of the interpreted Poole Sandstone interval in this well (827–877 m according to Reeckmann and Mebberson, 1984). The limestone overlies grey shale, attributed to the Grant Group, and includes, in the basal section, large clasts of mudstone. The limestone is approximately 7.5 m thick based on the wireline logs, and in core 1 consists of centimetre-scale interbeds of bryozoan-rich packstone–wackestone and intraclastic grainstone–rudstone (Fig. 11). Several very thin interbeds of fine-grained quartz sandstone–siltstone are present (Fig. 12). The biogenic material in the limestone is dominated by bryozoan fragments (Fig. 12), with crinoids generally rare but common to abundant only in a few narrow intervals. Brachiopods are generally rare but persistent throughout the core, less persistent are

This is an author-produced, peer-reviewed version of this article. The final, definitive version of this document can be found online at *Palaeogeography, Palaeoclimatology, Palaeoecology*, published by Elsevier. Copyright restrictions may apply. doi: 10.1016/j.palaeo.2014.05.009

foraminifera and *Tubiphytes* (Fig. 7D,E), with very rare echinoid spines, bivalve fragments showing prismatic microstructure, ostracod valves, gastropods and solitary corals also present (Fig. 12). Cyanobacterial borings into skeletal material are minor, and no micritic envelopes are developed around any of the grains. Some of the intraclasts are *Tubiphytes* boundstone. The matrix in the wackestone–packstone intervals has a clotted micritic texture in places.

Delicate Fenestrata dominate among the bryozoans in the Perindi 1 core, with robust Fenestrata less conspicuous, and arborescent rhabdomesid Cryptostomata and Trepostomata (dyscritellids and stenoporids) subordinate. Outsize fragments of the hexagonellid Cystoporata (*Evactinostella* and *Hexagonella*) occur sporadically.

Calcivertellines dominate the foraminiferal assemblage in Perindi 1. Among these, many *Trepeilopsis* morphotypes (Fig. 9A8) with matrix-filled central cavities are present together with *Calcitornella* morphotypes (Fig. 9A3) encrusting mainly bryozoan, crinoid and brachiopod debris. Lagenids are less common (mainly *Protonodosaria*), and tetrataxaceans (Fig. 9E3), endothyraceans (Fig. 9D2), pseudoammodiscids (Fig. 9G2–G3), and possible lasiodiscids (Fig. 9F3) are very rare.

In outcrop the most diverse components of the macrofossil assemblage so far identified include 10 bryozoan species, 14 brachiopod species, 34 bivalve species, and 15 gastropod species, with ammonoids, conulariids and plants also present (Skwarko, 1993). Crespin (1958) recorded four species of foraminifera from outcrop of the Nura Nura Member, including one *Calcitornella*, one *Hemigordius*, and two organic-cemented siliceous agglutinated foraminifera. A further two lagenid representatives were found in sub-surface sections of the member.

5.3 Age

This is an author-produced, peer-reviewed version of this article. The final, definitive version of this document can be found online at *Palaeogeography, Palaeoclimatology, Palaeoecology*, published by Elsevier. Copyright restrictions may apply. doi: 10.1016/j.palaeo.2014.05.009

Metalegoceras clarkei Miller, *Metalegoceras striatum* Teichert, *Thalassoceras wadei* Miller and *Propopanoceras ruzhencevi* Glenister and Furnish have been described from the type area of the Nura Nura Member (Miller, 1936; Teichert, 1942; Glenister and Furnish 1961; Glenister et al., 1993). These ammonoids are regarded as belonging to the late Sakmarian (Leonova, 1998, 2011; Boiko et al., 2008).

6. Southern Carnarvon Basin

6.1 Overview of Sakmarian–lower Artinskian sequence

During the Early Permian an elongate depocentre formed along the eastern margin of the Southern Carnarvon Basin (Hocking et al., 1987; Mory and Haig, 2011) as a series of half grabens, extending south to the eastern edge of the northern Perth Basin (see 7.1; Fig. 1). The Sakmarian–early Artinskian depositional sequence (Fig. 13) was initiated by marine flooding following deposition of the glacially-influenced Lyons Group. From the basal beds, the sequence shows an overall progradational trend that is terminated by renewed marine-flooding at the base of the Billidee Formation (here taken as the lower unit of the mainly upper Artinskian to Kungurian Byro Group which lies within the next major depositional sequence, Fig. 2).

Deposition of sheet-like beds extending great distances took place on a very low-gradient seafloor (Dixon and Haig, 2004; Haig, 2004; Mory and Haig, 2011). Beds are arranged in cycles that form shale to packstone/grainstone/quartz-sandstone units within the fully marine parts of the sequence (Fig. 14), and are interpreted as shoaling upward parasequences. Throughout most of the basin, the upper part of the sequence is made up of coarse-grained sandstone of the Wooramel Group ranging in origin from marginal-marine in

This is an author-produced, peer-reviewed version of this article. The final, definitive version of this document can be found online at *Palaeogeography, Palaeoclimatology, Palaeoecology*, published by Elsevier. Copyright restrictions may apply. doi: 10.1016/j.palaeo.2014.05.009

the north and at least partly fluvio-deltaic in the south. Within the sequence, limestone interbedded with mudstone or fine-grained sandstone characterises the Callytharra Formation (Condon, 1967; Hocking et al., 1987; Mory and Backhouse, 1997; Dixon and Haig, 2004; Frank et al., 2012).

No glacial influence is present within the sequence. Frank et al. (2012, fig. 2) showed an interval of "glacial influence" corresponding to the Winnemea and Ballythanna Sandstones based apparently only on correlation to the High Cliff Sandstone in the Perth Basin. The latter unit lacks the criteria for glaciation outlined by Fielding et al. (2008b, p. 130–132) as discussed here in 7.1.

6.2 Limestone composition

Limestones of the Callytharra Formation were examined in four outcrop sections:

1) a northernmost section adjacent the Lyndon River (Fig. 15; location 4 in Fig. 1);

2) about 72 km south in a composite section at Dead Man's Gully (Figs. 14, 16; location 5 in Fig. 1; Mory and Haig, 2011);

3) a further 120 km south, in a section in the Jimba Jimba area, (Fig. 17; location 6 in Fig. 1; Mory and Backhouse, 1997); and

4) in the type section of the Callytharra Formation, 113 km southeast of the Jimba Jimba Anticline (Fig. 18; location 7 in Fig. 1; Dixon and Haig, 2004).

Limestone low in the Callytharra Formation tends to be packstone in beds less than 50 cm thick. Those in the upper depositional cycles are generally grainstone and may be up to 1.5 m thick. Variable amounts of quartz and siliciclastic mud are present in the limestone beds. Quartz is particularly conspicuous in the interval from 40 m to 60 m in the Dead Man's

This is an author-produced, peer-reviewed version of this article. The final, definitive version of this document can be found online at *Palaeogeography, Palaeoclimatology, Palaeoecology*, published by Elsevier. Copyright restrictions may apply. doi: 10.1016/j.palaeo.2014.05.009

Gully section (Fig. 16) and may correlate with the Winnemea Sandstone Member in the Jimba Jimba area (Figs 13, 17).

Bryozoan fragments dominate the biogenic grain assemblage (Figs 15–18). Crinoids are common to abundant in many beds; and brachiopod debris is abundant to rare. Rare components of the assemblage include foraminifera, bivalve fragments with prismatic microstructure, ostracod valves, echinoid species, *Tubiphytes*, trilobite carapace debris, gastropods and solitary rugose corals. None of the grains have micritic envelopes and no cyanobacteria-encrusted grains are present. Ooids and microbialites are absent. In our material we did not find calcareous sponge spicules as reported by Frank et al. (2012) from subsurface sections of the Callytharra Formation.

The Bryozoa include a high diversity fauna dominated by Fenestrata and rhabdomesid Cryptostomata. In the upper part of the Callytharra Formation, large colonies of hexagonellid Cystoporata are conspicuous (viz. *Evactinostella* and *Hexagonella*). The Foraminifera are dominated by calcivertellines and lagenids (mainly *Protonodosaria*). Among the calcivertellines, *Trepeilopsis* morphotypes (Fig. 9A9–10) with matrix-filled central cavities and *Calcitornella* morphotypes (Fig. 9A4–6) encrusting bryozoan, crinoid and brachiopod debris are present. Hemigordiopsids (Fig. 9B4–6) are less common, and meandrospirines (Fig. 9C1–2) are very rare and found only in the northern sections. Simple representatives of the Fusulinida are very rare and include mainly pseudoammodiscids (Fig. 9G4–G8). Although tetrataxaceans and endothyraceans were not found in our acetate peels or thin sections, very rare specimens have been recorded from friable interbeds in the Callytharra Formation (Crespin, 1958; Dixon and Haig, 2004).

In addition to the groups identified here among the biogenic grains, tabulate corals, ammonoids, nautiloids, conulariids, annelids (*Spirorbis*), and plants have been reported from the formation (Skwarko, 1993). Among grains identified as crinoids, blastoids may also be

This is an author-produced, peer-reviewed version of this article. The final, definitive version of this document can be found online at *Palaeogeography, Palaeoclimatology, Palaeoecology*, published by Elsevier. Copyright restrictions may apply. doi: 10.1016/j.palaeo.2014.05.009

present as five species of this group have been identified from macrofossil remains. The most diverse macrofossil groups identified from the Callytharra Formation include 42 brachiopod species, 28 bryozoan species, 27 bivalve species, and 15 crinoid species (Skwarko, 1993).

A diverse assemblage of foraminifera belonging to miliolids (calcivertellines, hemigordiopsids and meandrospirines), lagenids (ichthyolariids and syzraniids), and organic-cemented siliceous agglutinated species have previously been recorded and illustrated from the Callytharra Formation (Crespin, 1958; Dixon and Haig, 2004). These came mainly from friable mudstone interbeds.

6.3 Age

Very few ammonoid specimens have been found in the Callytharra Formation and none from the type section. *Uraloceras irwinense* (Teichert and Glenister), *Metalegoceras* sp., *Mescalites* sp., and *Pseudohistoceras*? spp. have been identified (Glenister and Furnish, 1961; Cockbain, 1980; Glenister in Skwarko, 1993; Leonova, 1998; Mory and Haig, 2011). *Uraloceras irwinense* suggests a Sakmarian age although the genus is also known from the Artinskian (Leonova, 1998; 2011). *Metalegoceras* and *Mescalites* suggest a general Sakmarian–Artinskian age, but if the specimens from 60–70 m in the Dead Man's Gully section also include *Pseudohistoceras* (as tentatively suggested by T. Leonova, pers. comm. to M. Dixon, 2005) then these would indicate an Artinskian age for this interval (based on generic ranges described by Leonova, 2011). *Pseudohistoceras simile* Teichert, recorded from the lower Wooramel Group above the Callytharra Formation (Cockbain, 1980), indicates an Artinskian age for that level (see discussion in Appendix B, Supplementary Materials). The overlying lower part of the Byro Group (including Billidee Formation) contains late

This is an author-produced, peer-reviewed version of this article. The final, definitive version of this document can be found online at *Palaeogeography, Palaeoclimatology, Palaeoecology*, published by Elsevier. Copyright restrictions may apply. doi: 10.1016/j.palaeo.2014.05.009

Artinskian ammonoids representative of Leonova's (2011) *Neocrimites fredericksi–Medlicottia orbignyana* Zone (see Appendix B, Supplementary Materials).

Conodonts have not been recorded from any of the sections of Callytharra Formation studied here. However, in the upper part of the formation about 14 km north of locality 5 (Fig. 1), Nicoll and Metcalfe (1998) found a limited assemblage that was attributed to their *Mesogondolella bisselli–Sweetobnathus inornatus* Zone, including *Vjalovognathus australis*, known also in the Maubisse Limestone in Timor and considered to be late Sakmarian to Artinskian.

7. Northern Perth Basin

7.1 Overview of upper Sakmarian–lower Artinskian sequence

In the broader northern Perth Basin (Mory and Iasky, 1996) the Irwin River area is the southern-most of the contiguous Permian depocentres that trend south from the eastern part of the Southern Carnarvon Basin (Fig. 1). The depocentres are bounded on the east and west by major faults and, in part, by Proterozoic basement highs to the west. Coeval facies in the southern Perth Basin are non-marine.

The upper Sakmarian–lower Artinskian depositional sequence (Fig. 13) has an overall progradational trend from fully marine at the base to non-marine at the top. The lower 500 m of the section is composed mainly of marine mudstone (Holmwood Shale of Clarke et al., 1951). A thin calcareous mudstone unit in the lower part of the mudstone succession containing a monospecific assemblage of large ammonoids (*Juresanites*), has been designated the Beckett Member (Playford et al., 1976). Near the top of the Holmwood Shale discontinuous nodular limestone beds and highly fossiliferous friable sandy mudstones form

This is an author-produced, peer-reviewed version of this article. The final, definitive version of this document can be found online at *Palaeogeography, Palaeoclimatology, Palaeoecology*, published by Elsevier. Copyright restrictions may apply. doi: 10.1016/j.palaeo.2014.05.009

the Fossil Cliff Member (Clarke et al., 1951; Playford et al., 1976). Shoreface to marginal-marine facies of the High Cliff Sandstone progrades over the Holmwood Shale and is a transitional unit between the Holmwood Shale and the Irwin River Coal Measures in the uppermost part of the sequence (Mory and Haig, 2011).

The sequence lacks unambiguous evidence for glaciation (following criteria outlined by Fielding et al., 2008b). The rare discontinuous conglomeratic horizons in sandstone in the upper part of the High Cliff Sandstone type section (see Eyles et al., 2006) cannot be interpreted as dropstones but may be reworked older glacial material transported to the depositional site by debris flows. The type section is 3 km west of the Darling Fault that bounds the basin and was active during the Early Permian creating a depocentre west of the Yilgarn Precambrian Craton.

7.2. Limestone composition in Fossil Cliff Member

Nodular limestone from the Fossil Cliff Member was examined from two localities, 7.5 km apart (8 on Fig. 1) including the upper part of the type section of the Holmwood Shale (designated by Playford et al., 1976) and the type section of the Fossil Cliff Member. Limestone samples from the latter section are quartz-rich and include abundant brachiopod and bryozoan debris, and less common crinoidal plates, foraminifera and ostracods. In the upper part of the Holmwood Shale type section, the limestone usually has a siliciclastic mud matrix and contains abundant bryozoan fragments, brachiopod debris, foraminifera, crinoid plates, ostracod valves, and gastropods.

Foraminifera in the limestone samples are dominated by calcivertellines (Fig. 9A7, 11, 12), with less common hemigordiopsids (Fig. 9B7, 8) and lagenids (ichthyolariids and syzraniids). Organic-cemented siliceous agglutinated species and tetrataxids were previously

This is an author-produced, peer-reviewed version of this article. The final, definitive version of this document can be found online at *Palaeogeography, Palaeoclimatology, Palaeoecology*, published by Elsevier. Copyright restrictions may apply. doi: 10.1016/j.palaeo.2014.05.009

recorded and illustrated from friable beds of the Fossil Cliff Member by Crespin (1958) and Foster et al. (1985). Among the bryozoan grains observed in the nodular limestone, delicate Fenestrata are abundant; and arborescent Cryptostomata and robust Fenestrata are also conspicuous. Trepostomata (mainly encrusting taxa) are rare and Cystoporata have not been observed. Among the diverse macrofossil assemblage listed by Skwarko (1993) from the Fossil Cliff Member are five species of solitary-rugose and tabulate corals, five species of Bryozoa, 18 species of Brachiopoda, 40 species of Bivalvia, 19 species of Gastropoda, four species of nautiloids, one ammonoid, one trilobite, and three crinoid species.

7.3. Age

The ammonoid *Juresanites* is present at two levels in the lower Holmwood Shale and in the upper of these, it is found with *Uraloceras*. This association indicates a Sakmarian age for the lower Holmwood Shale (Glenister and Furnish, 1961; Leonova, 1998, 2011). A single specimen described as *Metalegoceras kayi* Glenister, Windle and Furnish (1973) from the Fossil Cliff Member is most similar to *M. distale* Ruzhencev, which is considered late Sakmarian (Glenister and Furnish, 1961; Boiko, et al., 2008).

8. Limestone Comparison

8.1 Age and sequence development

The available biostratigraphic evidence suggests that the late Sakmarian – early Artinskian is represented in each section of our study. The Maubisse Limestone probably represents the thickest single carbonate accumulation in the Permian of Timor, and is bounded

This is an author-produced, peer-reviewed version of this article. The final, definitive version of this document can be found online at *Palaeogeography, Palaeoclimatology, Palaeoecology*, published by Elsevier. Copyright restrictions may apply. doi: 10.1016/j.palaeo.2014.05.009

by volcaniclastic–siliciclastic units. Because the latter are, at present, poorly known, the position of the Maubisse Limestone within a broader depositional sequence is uncertain. The Australian sections show similarity in sequence development. Each sequence in the Southern Carnarvon and northern Perth Basins overlies units considered to exhibit some glacial influence. In the lower part of the sequence at each locality, calcareous marine beds are present. General progradational trends are recognized at each locality, and transition to marginal-marine or non-marine strata at the top of the sequence. In addition there is a consistent north–south trend of decreasing marine influence in the upper beds. There is no evidence (e.g. dropstones) for glacial sedimentation at any of the localities within the sequence. Marine flooding terminates the sequence with overlying marine shale at most localities. In the Merlinleigh and Irwin sub-basins, the overlying beds contain dropstones indicating amelioration of climate.

The problems with precise correlation of the sections include: (1) scarcity of conodonts in all formations studied; (2) absence of recoverable ammonoids in the type section of the Maubisse Formation and their great rarity in the Australian sections; and (3) the lack of age-diagnostic fusulinids in any section. Correlation of the Australian sections essentially depends on rare ammonoids. Because the record is so poor, no phylogenetic series of ammonoids can be recognized in the Australian successions that could test such assumptions made, for example, by Boiko et al. (2008) and their age implications. Therefore, even the discrimination between Sakmarian and Artinskian in the study region must be viewed with reservation (see discussion in Appendix B, Supplementary Materials). However, the biostratigraphic control for the studied sections is much stronger than for the upper Sakmarian to lower Artinskian deposits of eastern Australia which lack ammonoids and are correlated using endemic brachiopod faunas and palynofloras (Fielding et al. 2008b; Waterhouse and Shi, 2013).

This is an author-produced, peer-reviewed version of this article. The final, definitive version of this document can be found online at *Palaeogeography, Palaeoclimatology, Palaeoecology*, published by Elsevier. Copyright restrictions may apply. doi: 10.1016/j.palaeo.2014.05.009

8.2. Stratigraphic patterns

The Maubisse Limestone type section has an almost continuous ~180 m thick succession of limestone beds with few siliciclastic interbeds. Stratigraphically continuous limestone is also apparent in the short interval cored in Perindi 1, the most northern of the Australian sections examined here and that closest to the axis of the East Gondwana rift system. In contrast, limestone beds at the localities in the more restricted southern basins are mainly less than 1 m thick and interbedded within thicker friable mudstone units in a cyclic pattern. In the upper parts of the limestone sections, the mudstone to limestone cycles prograde forming units, several metres thick, containing several amalgamated limestone beds (Fig. 14).

The Maubisse Limestone type section and the Perindi 1 section may represent broad very shallow-marine bryozoan-dominated mound deposits. Outcrop of the Maubisse Formation near its type locality (Figs. 4, 5) suggest lateral changes in thickness, perhaps indicating a large lenticular body. The balance between carbonate build-up and available accommodation remained almost constant during deposition. This implies any subsidence contemporaneous with build-up negated eustatic effects and kept the depositional surface in the uppermost neritic zone (see 8.2). There may have been significant topographic relief between mounds and adjacent basinal areas but this cannot be ascertained on present data. However, the variety of Sakmarian–Artinskian carbonate facies in the Bisnain area of West Timor (Archbold and Barkham, 1989; Charlton et al., 2002) supports this hypothesis.

In the inner Canning Basin (locality 3, Fig. 1) and in the Southern Carnarvon Basin, the depositional cyclicity indicates that water depths periodically changed. Here the carbonate deposits, which form the tops of cycles, were sheet-like detrital accumulations over a very

This is an author-produced, peer-reviewed version of this article. The final, definitive version of this document can be found online at *Palaeogeography, Palaeoclimatology, Palaeoecology*, published by Elsevier. Copyright restrictions may apply. doi: 10.1016/j.palaeo.2014.05.009

shallow, low relief, seafloor (Dixon and Haig, 2004). Slight imbalances between subsidence and eustatic change during deposition may have produced the cyclic pattern.

In the Irwin River area, the paucity of limestone throughout the Holmwood Shale implies more restricted marine conditions with large freshwater influx into the basin, bringing an abundant supply of mud derived from a previously glaciated landscape. The thickness of the Sakmarian–Artinskian succession is greater than in the Merlinleigh Sub-basin to the north indicating varying accommodation along the Early Permian rift.

8.3. Limestone composition

Overall, the biogenic component of the limestone is similar through all basins. Bryozoan debris dominates the grain assemblage and is accompanied by common crinoidal plates, less common brachiopod debris, and rare foraminifera, ostracods, fragments of bivalve shells with prismatic microstructure, gastropods, echinoid spines, trilobite carapace fragments, and solitary rugose corals. *Tubiphytes* is present in variable abundance at all localities except in the marginal marine type section of the Nura Nura Member in the inner Canning Basin and in the Irwin River area, the southern most of the basins studied (Fig. 19). Absent from the limestone at each locality are grains with micritic envelops (cortoids), cyanobacterial encrustations, peloids, ooids, oncoids, and microbialites.

Much more taxonomic study is needed on the Bryozoa in order to make comparisons between those assemblages. The megaloscopic hexagonellid cystoporata so conspicuous in the Western Australian basins (viz. *Evactinostella* and *Hexagonella*) appear to be totally absent from the type section of the Maubisse Limestone in Timor. This probably is due to differences in ecological setting as described in 8.2.

Significant similarities in foraminiferal assemblages exist between the Maubisse Limestone and localities 2 and 4–7 in the south (Fig. 19). No complex fusulinids are present

This is an author-produced, peer-reviewed version of this article. The final, definitive version of this document can be found online at *Palaeogeography, Palaeoclimatology, Palaeoecology*, published by Elsevier. Copyright restrictions may apply. doi: 10.1016/j.palaeo.2014.05.009

and the assemblages are dominated by calcivertellines. Among the latter are *Trepeilopsis* morphotypes with matrix-filled central cavities suggesting, as Dixon and Haig (2004) deduced, that these tests were attached to algal macrophytes that decayed either before or shortly after burial. Simple fusulinids, including endothyraceans, tetrataxaceans and pseudoammodiscids extend far south, whereas lasiodiscids are confined to the northern localities.

Tubiphytes was previously recorded from upper Sakmarian limestone in West Timor (Riding and Barkham, 1999, as *Shamovella*) associated with a bryozoan–crinoid dominated assemblage. It is here recorded for the first time in west Australian upper Sakmarian–lower Artinskian limestone as far south as the southern end of the Southern Carnarvon Basin (locality 7, type section of Callytharra Formation).

8.4 Paleobathymetry

Stemmerik's (1997) paleobathymetric model for Permian cool-water carbonate facies in northern Pangea, based on a modern analogue along the southern Australian shelf, does not apply to the carbonate accumulations studied here. Temperate carbonate deposits on the narrow passive-margin shelves of south and southwest Australia, described by James et al. (1992, 1999), are influenced by high-energy open shelf conditions with a deep (<100 m) storm-wave base. By contrast the studied carbonate accumulations were deposited within Sakmarian–Artinskian intracratonic basins that were, at least in the Southern Carnarvon and northern Perth Basins, narrow, very shallow seaways with a very shallow storm-wave base (Haig, 2003, 2004; Dixon and Haig, 2004). The detrital sheet-like carbonate deposits at the tops of shale to limestone cycles probably accumulated above the shallow storm-wave base.

This is an author-produced, peer-reviewed version of this article. The final, definitive version of this document can be found online at *Palaeogeography, Palaeoclimatology, Palaeoecology*, published by Elsevier. Copyright restrictions may apply. doi: 10.1016/j.palaeo.2014.05.009

Indirect evidence for organisms that required photosynthesis to live is provided by borings attributed to cyanobacteria, probably representing holdfasts for filamentous types growing on skeletal debris, and in the central cavities in the encrusting miliolid foraminifera *Trepeilopsis* that may reflect algal macrophytes around which the coils of *Trepeilopsis* encrusted. The presence of such photosynthetic organisms indicates water depths probably in the inner neritic zone (Dixon and Haig, 2004). The dominance of large encrusting porcellaneous calcivertellines among the foraminifera also indicates very shallow water based on modern encrusting porcellaneous foraminifera with similar growth forms (e.g. the nubeculariids in the south-west Australian inner neritic zone; Semeniuk 2000, 2001).

9. Comparison with eastern Australian succession

The Early Permian basins of eastern Australia lay at the margin of eastern Gondwana (Fielding et al., 2008b, fig. 3B) in contrast to the west Australian basins that lay in the interior of Gondwana along the east Gondwana interior rift system. No intracratonic seaway crossed the continent to connect eastern and west Australian basins. Even though basins in Queensland and New South Wales were positioned at the same 45°–60°S paleolatitudes as the Southern Carnarvon and Perth Basins in Western Australia, the basins on each side of the continent were subjected to different oceanographic influences with eastern Australian basins adjacent hinterland areas with much greater topographic relief (along earlier Paleozoic orogenic belts). The Permian of Tasmania was deposited at a paleolatitude of about 70°S (James et al., 2009, fig. 1B).

Fielding et al. (2008a,b,c, 2010) defined four glaciations separated by non-glacial intervals in the Permian of eastern Australia. Based on their time scale, the upper Sakmarian to lower Artinskian interval studied here apparently corresponds to glaciation P2 in eastern

This is an author-produced, peer-reviewed version of this article. The final, definitive version of this document can be found online at *Palaeogeography, Palaeoclimatology, Palaeoecology*, published by Elsevier. Copyright restrictions may apply. doi: 10.1016/j.palaeo.2014.05.009

Australia (although Waterhouse and Shi, 2013, fig. 4, suggested that there may be a problem with the chronostratigraphic position of P2). The stage correlations for the eastern Australian P2 formations were based on endemic brachiopod zones and palynofloras, and Fielding et al. (2008a,b, 2010) did not explain the levels of uncertainty in these correlations.

James et al. (2009) recognized no carbonate units in P2. Below P2 in the non-glacial interval above Asselian to early Sakmarian P1, limestone is represented in the Lower Parmeener Supergroup in Tasmania (Rogala et al., 2007; James et al., 2009; Fielding et al., 2010; Reid, 2010; Isbell et al., 2013). In the correlation advanced by Fielding et al. (2008a,b), this limestone was placed in the middle Sakmarian and includes argillaceous rudstone, floatstone and grainstone with thick-shelled bivalves and brachiopods and bryozoans as the main components, and minor crinoid debris. The bioclastic assemblage contrasts with the dominance of bryozoa and crinoids in the western Australian carbonate deposits of late Sakmarian to early Artinskian age. The Tasmanian limestone facies also contain abundant dropstones and include spiculitic limestone preserved in phosphatic nodules. Crespin (1958) recognized that the foraminifera from this level in Tasmania were similar to those from the Fossil Cliff Member, Callytharra Formation and Nura Nura Member of Western Australia, but lack endothyraceans, tetrataxaceans, and pseudoammodiscids present in Western Australia (this study). *Tubiphytes* has not been found in the Sakmarian limestone in Tasmania, but is present in the Callytharra Formation of Western Australia (see 6.2). Based on sedimentological and paleontological differences, it appears that the Sakmarian limestone in Tasmania was deposited in much cooler water than the west Australian late Sakmarian–early Artinskian deposits.

The late Artinskian to early Kungurian interval between glaciations P2 and P3 was the time of significant carbonate deposition in the eastern Australian basins (Fielding et al., 2008a,b; James et al., 2009; Clapham and James, 2012, fig. 7). The chronostratigraphic

This is an author-produced, peer-reviewed version of this article. The final, definitive version of this document can be found online at *Palaeogeography, Palaeoclimatology, Palaeoecology*, published by Elsevier. Copyright restrictions may apply. doi: 10.1016/j.palaeo.2014.05.009

correlation is supported by one radiometric date (Roberts et al., 1996) and rare ammonoids that Leonova (2011) regarded as Kungurian. The biogenic component of the carbonate lithofacies recorded by James et al. (2009) includes bryozoans, brachiopods, bivalves, crinoids, sponge spicules, tabulate corals, solitary rugose corals, gastropods, porcellaneous foraminifera including mainly *Calcitornella* (wrongly classified as "porcellaneous endothyrids" by James et al., 2009, p. 129) and hyaline foraminifera (lagenids). Minor *Tubiphytes* was found in limestone from the northern-most basin studied by James et al. (2009). In general terms, the composition of the upper Artinskian–lower Kungurian limestone facies in eastern Australia resembles that of the Callytharra Formation in the Southern Carnarvon Basin.

No significant carbonate units are known from the late Artinskian to early Kungurian interval in Western Australian Basins. As outlined in Figs. 2, 13 and Appendix B (Supplementary Materials), during this time siliciclastic facies with prominent mud–sand cyclicity were deposited (viz. lower Byro Group in the Southern Carnarvon Basin, lower Carynginia Formation in the northern Perth Basin, and lower Noonkanbah Formation in the Canning Basin). In Timor, we have recently found fusulinid limestones that may belong within this time interval. The lowermost Byro Group and lowermost Carynginia Formation contain scattered dropstones indicating cool-water conditions where sea ice was present. Higher in the lower Byro Group, brachiopods indicate warming conditions reaching a maximum in the Bulgadoo–Cundlego sequence (Fig. 13, Appendix B, Supplementary Materials) where there is an influx of Tethyan genera (Archbold and Shi, 1995). Therefore, although there are no carbonate deposits in the Western Australian basins, there is correspondence with the eastern Australian succession in a warm latest Artinskian–early Kungurian interval. The siliciclastic content of the west Australian basins probably reflects a

This is an author-produced, peer-reviewed version of this article. The final, definitive version of this document can be found online at *Palaeogeography, Palaeoclimatology, Palaeoecology*, published by Elsevier. Copyright restrictions may apply. doi: 10.1016/j.palaeo.2014.05.009

greater influx (at least periodically) of sediment-laden freshwater into the shallow seas (Haig, 2003, 2004) that was climatically driven.

Within the Asselian to early Kungurian interval in both eastern and western Australian successions, two cool to cold phases are recognized separated by a warmer interval, and followed by a final warm phase (Fig. 20). The initial cold phase and the final warm phase are synchronous in both regions (viz. Asselian–early Sakmarian and late Artinskian–early Kungurian, respectively). Differences are with chronostratigraphic correlations of (1) the late Sakmarian–early Artinskian warmer phase identified in the west Australian succession and the interval between glaciations P1 and P2 in eastern Australia; and (2) the subsequent cool phase in west Australia and glaciation P2 in eastern Australia. Perhaps non-glacial P1–P2 phase corresponds to the Ist post-glacial depositional cycle we recognize in the west Australian succession (Figs. 2,13) and which we consider from ammonoid evidence to be late Sakmarian to early Artinskian. Glaciation P2 may correspond to the cool interval represented at the base of the Byro Group and the basal Carynginia Formation that we place in the "mid" Artinskian (see Fig. 13; Appendix B, Supplementary Material). The eastern Australian basins may have been influenced by alpine glaciation and therefore experienced more pronounced and prolonged glacial episodes than those that affected west Australian basins. However, although glacioeustacy may have influenced depositional cyclicity in the west Australian basins (e.g. Southern Carnarvon Basin studies by Lever, 2004, for the Roadian Kennedy Group and Haig, 2003, for the Kungurian Quinnanie Shale) there is no evidence for fluvial incision anywhere in the post-Lower Sakmarian succession that would indicate abrupt lowering of sea-level.

10. Discussion

This is an author-produced, peer-reviewed version of this article. The final, definitive version of this document can be found online at *Palaeogeography, Palaeoclimatology, Palaeoecology*, published by Elsevier. Copyright restrictions may apply. doi: 10.1016/j.palaeo.2014.05.009

This study has examined inner neritic limestone deposited in an interior rift system trending approximately north to south for about 2000 km through a paleolatitudal range from about 35°S to higher than 55°S (following Li and Powell, 2001). These Sakmarian–Artinskian carbonate deposits are dominated by heterozoan elements (following the classification of James, 1997), and indicate temperate marine conditions. Tropical elements such as larger fusulinids, colonial rugose corals, and dasycladacean algae are absent as are cortoidal grains, cyanobacteria-encrusted grains, ooids, oncoids, and microbialites. The dominance of miliolid species among the foraminiferal assemblage, with calcified skeletons of bryozoans, brachiopods and echinoderm groups (which together indicate salinity tolerances of 30–50 psu; Mossadegh et al., 2009) and the absence of common metahaline–hypersaline indices such as cortoids, cyanobacteria-encrusted grains, ooids and microbialites indicate normal salinity conditions during limestone deposition.

The problematic group *Tubiphytes* (as interpreted by Senowbari-Daryan, 2013) has been found as far south as about 55°S paleolatitude in the interior-rift system (in the southern part of the Southern Carnarvon Basin), and smaller fusulinids belonging to the endothyraceans, tetrataxaceans and pseudoammodiscids also have an extended north–south range (Fig. 19). An aspect of *Tubiphytes* physiology apparent from our material was the ability of this organism to secrete its microgranular skeleton in the very fine interstices within the lattice of crinoid columnals (e.g. Fig. 7B), a feature also shown by calcivertelline foraminifera (e.g. Fig. 9A5).

Oxygen-isotope paleothermometry on brachiopod shells from the Callytharra Formation in the Southern Carnarvon Basin indicates cool temperate conditions <10°C (Compston, 1960; Korte et al., 2008; Frank et al., 2012; Mii et al., 2012). Korte et al. (2008) indicated a 9–12°C gradient between <30°S and 45–65°S paleolatitude, which is less than the modern equivalent gradient of about 15°C. The biogenic grain composition in limestones over

This is an author-produced, peer-reviewed version of this article. The final, definitive version of this document can be found online at *Palaeogeography, Palaeoclimatology, Palaeoecology*, published by Elsevier. Copyright restrictions may apply. doi: 10.1016/j.palaeo.2014.05.009

the 35°–55° paleolatitude range examined here also indicates a low temperature gradient. The lack of tropical indicators in the most northern locality (Maubisse Limestone type section) suggests a paleotemperature of <18° C (the modern lower limit of coral–algal reef development along the present west Australian coast; Hatcher, 1991).

The absence of any reports of *Tubiphytes* and fusulinids such as endothyraceans, tetrataxaceans and pseudoammodiscids in Sakmarian–early Artinskian deposits from eastern Australia, suggests that water temperatures in the East Gondwana interior-rift system were higher than those in the epeiric seas of eastern Australia. Based on marine invertebrates, but in particular the brachiopods, Archbold and Shi (1995, 1996) recognized a Westralian biogeographic province for the late Sakmarian–Artinskian comprising faunas, including warm-water elements, from the Perth, Carnarvon and Canning Basins as well as from New Guinea (West Papua), Timor, and other blocks now within southern Asia. Coeval faunas from eastern Australia were distinguished as the Austrazean Province and regarded as indicative of extremely cold-water conditions (Archbold, 2000, 2001).

Reid and James (2010) recognized similarities between the Australian bryozoan faunas and those from high northern paleolatitudes. Shi and Grunt (2000) described a similar correspondence among the brachiopods. Lower Permian biogenic carbonates formed by heterozoan assemblages, similar to those studied here, are present within the intracratonic basins of northern Pangea (Beauchamp and Desrochers, 1997; Stemmerik, 1997). *Tubiphytes* is also present in some of the bryozoan-dominated limestones in these high-latitude northern basins. However, cold-water spiculitic facies, similar to those described by Ehrenberg et al. (2001) and Beauchamp and Baud (2002) from northern Pangea, have not been found in the Timor–west Australian basins.

11. Conclusions

This is an author-produced, peer-reviewed version of this article. The final, definitive version of this document can be found online at *Palaeogeography, Palaeoclimatology, Palaeoecology*, published by Elsevier. Copyright restrictions may apply. doi: 10.1016/j.palaeo.2014.05.009

The studied late Sakmarian–early Artinskian carbonate deposits accumulated in shallow seas that extended far into the interior of eastern Gondwana and show no glacial influence. The biogenic components of the sediment, which dominate the deposits, suggest temperate conditions with a low north to south temperature gradient. In more open-marine parts of the interior-rift system, carbonate mounds seem to have developed forming thick limestone successions, whereas in the more southerly basins sheet-like detrital carbonate deposits developed periodically in restricted waters above a very shallow storm-wave base.

The temperate late Sakmarian to early Artinskian interval represented in basins of the east Gondwana interior rift system may be equivalent to the non-glacial interval between glaciations P1 and P2 in eastern Australia, but further consideration of the chronostratigraphic correlation is required. The subsequent cool phase observed in the "mid" Artinskian of the west Australian basins may be equivalent to the more expansive and longer P2 glaciation in eastern Australia, but this correlation also requires further investigation.

11. Acknowledgements

Field work for this study was carried out over the last 10 years and we are grateful to the many people who have helped us with this work. Funding from Eni Australia and Eni Timor Leste, The University of Western Australia and Geoscience Australia supported our studies in Timor-Leste. The University of Western Australia and the Geological Survey of Western Australia have supported our work in the Australian basins. We are very grateful to various Government agencies in Timor-Leste who have supported and facilitated our field studies in their country since 2003. In particular, for our studies in the Maubisse area, we thank Manuel Ramos Pinto, District Administrator of Ainaro; Luis Casimiro Lopes, Subdistrict

This is an author-produced, peer-reviewed version of this article. The final, definitive version of this document can be found online at *Palaeogeography, Palaeoclimatology, Palaeoecology*, published by Elsevier. Copyright restrictions may apply. doi: 10.1016/j.palaeo.2014.05.009

Administrator of Maubisse; and Filomeno Maria Mendonca, Suco Chief of Maubisse. For valuable suggestions that have improved our manuscript we thank Finn Surlyk, Tim Charlton and an anonymous reviewer. VID was partly supported by NSF grant EAR-0746107. AJM publishes with the permission of the Director, Geological Survey of Western Australia.

12. References

Ali J.R., Aitchison, J.C., Chik, S.Y.S., Baxter, A.T., Bryan, S.E., 2013. Paleomagnetic data support Early Permian age for the Abor Volcanics in the lower Siang Valley, NE India: Significance for Gondwana-related break-up models. Journal of Asian Earth Sciences 50, 105–115.

Archbold, N.W., 2000. Palaeobiogeography of the Australasian Permian. Memoir of the Association of Australasian Palaeontologists 23, 287–310.

Archbold, N.W., 2001. Wallace lines in eastern Gondwana: Palaeobiogeography of Australasian Permian Brachiopoda. In: Metcalfe, I., Smith, J.M.B., Morwood, M., Davidson, I., (Eds.), Faunal and Floral Migrations and Evolution in SE Asia–Australasia. A.A. Balkema, Lisse, Germany, 73–83

Archbold, N.W., Barkham, S.T., 1989. Permian Brachiopoda from near Bisnain Village, West Timor. Alcheringa 13, 125–140.

Archbold, N.W., Hogeboom, T., 2000. Subsurface Brachiopoda from borehole cores through the Early Permian sequence of the Carnarvon Basin, Western Australia: correlations with palynological biostratigraphy. Proceedings of the Royal Society of Victoria 112, 93–109.

Archbold, N.W., Pigram, C.J., Ratman, N., Hakim, S., 1982. Indonesian Permian brachiopod fauna and Gondwana–South-East Asia relationships. Nature 296, 556–558.

This is an author-produced, peer-reviewed version of this article. The final, definitive version of this document can be found online at *Palaeogeography, Palaeoclimatology, Palaeoecology*, published by Elsevier. Copyright restrictions may apply. doi: 10.1016/j.palaeo.2014.05.009

Archbold, N.W., Shi, G.R., 1995. Permian brachiopod faunas of Western Australia: Gondwanan–Asian relationships and Permian climate. Journal of Southeast Asian Earth Sciences 11, 207–215.

Archbold, N.W., Shi, G.R., 1996. Western Pacific Permian marine invertebrate palaeobiogeography. Australian Journal of Earth Sciences 43, 635–641.

Audley-Charles, M.G., 1968. The geology of Portuguese Timor. Geological Society of London Memoir 4, 1–76.

Audley-Charles, M.G., 1983. Reconstruction of eastern Gondwanaland. Nature 306, 48–50.

Audley-Charles, M.G., 1984. Cold Gondwana, warm Tethys and the Tibetan Lhasa block. Nature 310, 165–166.

Audley-Charles, M.G., 1988. Evolution of the southern margin of Tethys (Northern Australian region) from early Permian to late Cretaceous. Geological Society Special Publication 37, 79–100.

Bassler, R.S., 1929. The Permian Bryozoa of Timor. Paläontologie von Timor 16, 37–90.

Beauchamp, B., Baud, A., 2002. Growth and demise of Permian biogenic chert along northwest Pangea: evidence for end-Permian collapse of thermohaline circulation. Palaeogeography, Palaeoclimatology, Palaeoecology 184, 37–63.

Beauchamp, B., Desrochers, A., 1997. Permian warm- to very cold carbonates and cherts in northwest Pangea. In: James, N.P. and Clarke, J.A.D. (Eds.), Cool-water carbonates. Society of Economic Paleontologists and Mineralogists, Special Publication 56, 327–347.

Boiko, M.S., Leonova, T.B., Lin, M., 2008. Phylogeny of the Permian Family Metalegoceratidae (Goniatitida, Ammonoidea). Paleontological Journal 42, 585–595.

Brouwer, H.A., 1942. Summary of the geological results of the expedition. In, Brouwer, H.A. (ed.), Geological Expedition of the University of Amsterdam to the Lesser Sunda Islands in the South Eastern Part of the Netherlands East Indies 1937, 4, 347–401.

This is an author-produced, peer-reviewed version of this article. The final, definitive version of this document can be found online at *Palaeogeography, Palaeoclimatology, Palaeoecology*, published by Elsevier. Copyright restrictions may apply. doi: 10.1016/j.palaeo.2014.05.009

Brunnschweiler, R.O., 1978. Notes on the geology of eastern Timor. Bureau of Mineral Resources, Geology and Geophysics, Australia, Bulletin 192, 241–259.

Carter, D.J., Audley-Charles, M.G., Barber, A.J., 1976. Stratigraphical analysis of island arc-continental margin collision in eastern Indonesia. Journal of the Geological Society of London 132, 179–198.

Chamalaun, F.H., 1977. Palaeomagnetic reconnaissance result from the Maubisse Formation, East Timor, and its tectonic implication. Tectonophysics 42, T17–T26.

Charlton, T.R., Barber, A.J., Harris, R.A., Barkham, S.T., Bird, P.R., Archbold, N.W., Morris, N.J., Nicoll, R.S., Owen, H.G., Owens, R.M., Sourauf, J.E., Taylor, P.D., Webster, G.D., Whittaker, J.E., 2002. The Permian of Timor: stratigraphy, palaeontology and palaeogeography. Journal of Asian Earth Sciences 20, 719–774.

Clapham, M.E., James, N.P., 2012. Regional-scale marine change in eastern Australia during Permian climate fluctuations and its relationship to local community restructuring. Palaios 27, 627–635.

Clarke, E. de C., Prendergast, K.L., Teichert, C., Fairbridge, R.W., 1951. Permian succession and structure in the northern part of the Irwin Basin, Western Australia. Journal and Proceedings of the Royal Society of Western Australia 35, 31–84.

Cockbain, A.E., 1980. Permian ammonoides from the Carnarvon Basin – a review. Geological Survey of Western Australia, Annual Report 1979, 100–105.

Compston, W., 1960. The carbon isotopic compositions of certain marine invertebrates and coals from the Australian Permian. Geochimica et Cosmochimica Acta 18, 1–22.

Condon, M.A., 1967. The geology of the Carnarvon Basin, Western Australia, Part 2: Permian stratigraphy. Bureau of Mineral Resources, Geology and Geophysics, Australia, Bulletin 77, 1–190.

This is an author-produced, peer-reviewed version of this article. The final, definitive version of this document can be found online at *Palaeogeography, Palaeoclimatology, Palaeoecology*, published by Elsevier. Copyright restrictions may apply. doi: 10.1016/j.palaeo.2014.05.009

Crespin, I., 1958. Permian Foraminifera of Australia. Bureau of Mineral Resources, Geology and Geophysics, Australia, Bulletin 48, 1–207.

Crostella, A.A., Powell, D.E., 1975. Geology and hydrocarbon prospects of the Timor area. Proceedings Indonesian Petroleum Association, Fourth Annual Convention 1975, 149–171.

Crowe, R.W.A., Towner, R.R., 1976. Environmental interpretation of the Permian Nura Nura Member of the Poole Sandstone, Noonkanbah Sheet Area, Canning Basin: A gradation between fluviatile and shallow-water marine facies. Geological Survey of Western Australia, Annual Report 1975, 59–62.

Davydov, V.I., Haig, D.W., McCartain, E., 2013. A latest Carboniferous warming spike recorded by a fusulinid-rich bioherm in Timor Leste: Implications for East Gondwana deglaciation. Palaeogeography, Palaeoclimatology, Palaeoecology 376, 22–38.

Dixon, M., Haig, D.W., 2004. Foraminifera and their habitats within a cool-water carbonate succession following glaciation, Early Permian (Sakmarian), Western Australia. Journal of Foraminiferal Research 34, 308–324.

Ehrenberg, S.N., Pickard, N.A.H., Henriksen, L.B., Svånå, Gutteridge, P., Macdonald, D., 2001. A depositional and sequence stratigraphic model for cold-water spiculitic strata based on the Kapp Starostin Formation (Permian) of Spitsbergen and equivalent deposits from the Barents Sea. AAPG Bulletin 85, 2061–2087.

Eyles, C.H., Eyles, N., 2000. Subaqueous mass flow origin for Lower Permian diamictites and associated facies of the Grant Group, Barbwire Terrace, Canning Basin, Western Australia. Sedimentology 47, 343–356.

Eyles, C., Mory, A.J., Eyles, N., 2003. Carboniferous–Permian facies and tectono-stratigraphic successions of the glacially influenced and rifted Carnarvon Basin, western Australia. Sedimentary Geology 155, 63–86.

This is an author-produced, peer-reviewed version of this article. The final, definitive version of this document can be found online at *Palaeogeography, Palaeoclimatology, Palaeoecology*, published by Elsevier. Copyright restrictions may apply. doi: 10.1016/j.palaeo.2014.05.009

Eyles, N., Mory, A.J., Eyles, C.H., 2006. 50-million-year-long record of glacial to postglacial marine environments preserved in a Carboniferous–Lower Permian graben, northern Perth Basin, Western Australia. Journal of Sedimentary Research 76, 618–632.

Fielding, C.R., Frank, T.D., Birgenheier, Rygel, M.C., Jones, A.T., Roberts, J., 2008a. Stratigraphic imprint of the Late Palaeozoic Ice Age in eastern Australia: a record of alternating glacial and nonglacial climate regime. Journal of the Geological Society of London 165, 129–140.

Fielding, C.R., Frank, T.D., Birgenheier, Rygel, M.C., Jones, A.T., Roberts, J., 2008b. Stratigraphic record and facies associations of the late Paleozoic ice age in eastern Australia (New South Wales and Queensland). Geological Society of America Special Publication 441, 41–57.

Fielding, C.R., Frank, T.D., Isbell, J.L., 2008c. The late Paleozoic ice age—A review of current understanding and synthesis of global climate patterns. Geological Society of America Special Publication 441, 343–354.

Fielding, C.R., Frank, T.D., Isbell, J.L., Henry, L.C., Domack, E.W., 2010. Stratigraphic signature of the late Palaeozoic Ice Age in the Parmeener Supergroup of Tasmania, SE Australia, and inter-regional comparisons. Palaeogeography, Palaeoclimatology, Palaeoecology 298, 70–90.

Flügel, E., 2004. Microfacies of Carbonate Rocks. Springer-Verlag, Berlin, 1–984.

Foster, C.B., Palmieri, V., Fleming, P.J.G., 1985. Plant microfossils, Foraminiferida, and Ostracoda, from the Fossil Cliff Formation (Early Permian, Sakmarian), Perth Basin, Western Australia. Special Publications of the South Australian Department of Mines nad Energy 5, 61–105.

This is an author-produced, peer-reviewed version of this article. The final, definitive version of this document can be found online at *Palaeogeography, Palaeoclimatology, Palaeoecology*, published by Elsevier. Copyright restrictions may apply. doi: 10.1016/j.palaeo.2014.05.009

Frank, T.D., Pritchard, J.M., Fielding, C.R., Mory, A.J., 2012. Cold-water carbonate deposition in a high-latitude, glacially influenced Permian seaway (Southern Carnarvon Basin, Western Australia). Australian Journal of Earth Sciences 59, 479–494.

Gageonnet, R., Lemoine, M., 1958. Contribution à la connaissance de la géologie de la province Portugaise de Timor. Estudos, Ensaios e Documentos, Junta de Investigações do Ultramar 48, 1–138.

Glenister, B.F., Furnish, W.M., 1961. The Permian ammonoides of Australia. Journal of Paleontology 35, 673–736.

Glenister, B.F., Rogers, F.S., Skwarko, S.K., 1993. Ammonoids. Geological Survey of Western Australia Bulletin 136, 54–63 (plus Appendix).

Glenister, B.F., Windle, D.L., Furnish, W.M., 1973. Australasian Metalegoceratidae (Lower Permian Ammonoids). Journal of Paleontology 47, 1031–1043.

Gorter, J.D., Poynter, S.E., Bayford, S.W., Caudullo, A., 2008, Glacially influenced petroleum plays in the Kulshill Group (Late Carboniferous– Early Permian) of the southeastern Bonaparte Basin, Western Australia. APPEA Journal 2008, 69–114.

Groves, J.R., Rettori, R., Altiner, D., 2004. Wall structures in selected Paleozoic lagenide foraminifera. Journal of Paleontology 78, 245–256.

Guppy, D.J., Lindner, A.W., Rattigan, J.H., Casey, J.N., 1958. The geology of the Fitzroy Basin, Western Australia. Bureau of Mineral Resources, Geology and Geophysics, Australia, Bulletin 36, 1–116.

Haig, D.W., 2003. Palaeobathymetric zonation of foraminifera from lower Permian shale deposits of a high-latitude southern interior sea. Marine Micropaleontology 49, 317–334.

Haig, D.W., 2004. Comparison of foraminifera and habitats from Australian Permian and Cretaceous interior seas. Memoirs of the Association of Australasian Palaeontologists 29, 31–46.

This is an author-produced, peer-reviewed version of this article. The final, definitive version of this document can be found online at *Palaeogeography, Palaeoclimatology, Palaeoecology*, published by Elsevier. Copyright restrictions may apply. doi: 10.1016/j.palaeo.2014.05.009

Hall, R., Sevastjanova, I., 2012. Australian crust in Indonesia. Australian Journal of Earth Sciences 59, 827–844.

Hamilton, W., 1979. Tectonics of the Indonesian region. US Geological Survey Professional Paper 1078.

Harrowfield, M., Holdgate, G., Wilson, C.J.L., McLoughlin, S., 2005. Tectonic significance of the Lambert graben, East Antarctica: Reconstructing the Gondwanan rift. Geology 33, 197–200.

Hatcher, B.G., 1991. Coral reefs in the Leeuwin Current – an ecological perspective. Journal of the Royal Society of Western Australia 74, 115–127.

Heine, C., Müller, R.D., 2005. Late Jurassic rifting along the Australian North West Shelf: margin geometry and spreading ridge configuration. Ausrtalian Journal of Earth Sciences 52, 27–39.

Hocking, R.M., Moors, H.T., van de Graaff, J.E., 1987. Geology of the Carnarvon Basin, Western Australia. Geological Survey of Western Australia Bulletin 133, 1–289.

Isbell, J.L., Henry, L.C., Reid, C.M., Fraiser, M.L., 2013. Sedimentology and palaeoecology of lonestone-bearing mixed clastic rocks and cold-water carbonates of the Lower Permian Basal Beds at Fossil Cliffs, Maria Island, Tasmania (Australia): Insight into the initial decline of the late Palaeozoic ice age. Geological Society, London, Special Publications 376, 307–341.

James N.P., 1997. The cool-water carbonate depositional realm. In: James, N.P. and Clarke, J.A.D. (Eds.), Cool-water carbonates. Society of Economic Paleontologists and Mineralogists, Special Publication 56, 1–20.

James, N.P., Bone, Y., von der Borch, C.C., Gostin, V.A., 1992. Modern carbonate and terrigenous clastic sediments on a cool-water, high-energy, mid-latitude shelf: Lacepede, southern Australia. Sedimentology 39, 877–903.

This is an author-produced, peer-reviewed version of this article. The final, definitive version of this document can be found online at *Palaeogeography, Palaeoclimatology, Palaeoecology*, published by Elsevier. Copyright restrictions may apply. doi: 10.1016/j.palaeo.2014.05.009

James, N.P., Collins, L.B., Bone, Y., Hallock, P., 1999. Subtropical carbonates in a temperate realm: modern sediments on the southwest Australian shelf. Journal of Sedimentary Research 69, 1297–1321.

James, N.P., Frank, T.D., Fielding, C.R., 2009. Carbonate sedimentation in a Permian high-latitude, subpolar depositional realm: Queensland, Australia. Journal of Sedimentary Research 79, 125–143.

Korte, C., Jones, P.J., Brand, U., Mertmann, D., Veizer, J., 2008. Oxygen isotope valvues from high-latitudes: Clues for Permian sea-surface temperature gradients and Late Palaeozoic deglaciation. Palaeogeography, Palaeoclimatology, Palaeoecology 269, 1–16.

Leonova, T.B., 1998. Permian ammonoids of Russia and Australia. Proceedings of the Royal Society of Victoria 110, 157–162.

Leonova, T.B., 2011. Permian ammonoids: biostratigraphic, biogeographical, and ecological analysis. Paleontological Journal 45, 1206–1312.

Lever, H., 2004. Climate changes and cyclic sedimentation in the Mid-Late Permian: Kennedy Group, Carnarvon Basin, Western Australia. Gondwana Research 7, 135–142.

Li, Z.X., Powell, C.McA., 2001. An outline of the palaeogeographic evolution of the Australasian region since the beginning of the Neoproterozoic. Earth Science Reviews 53, 237–277.

Loeblich, A.R., Tappan, H., 1987. Foraminiferal Genera and their Classification. Van Nostrand Reinhold Company, New York, 2 volumes, 1-970.

McCartain, E., Backhouse, J., Haig, D., Balme, B., Keep, M., 2006. Gondwana-related Late Permian palynoflora, foraminifers and lithofacies from the Wailuli Valley, Timor Leste. Neues Jahrbuch fur Geologie und Palaontologie, Abhandlungen 240, 53–80.

Meijer, H.J.M., Donovon, S.K., Renema, W., 2009. Major Dutch collections of Permian fossils from Timor amalgamated. Journal of Paleontology 83, 313.

This is an author-produced, peer-reviewed version of this article. The final, definitive version of this document can be found online at *Palaeogeography, Palaeoclimatology, Palaeoecology*, published by Elsevier. Copyright restrictions may apply. doi: 10.1016/j.palaeo.2014.05.009

Mii, H., Shi, G.R., Wang, C., 2012. Late Paleozoic middle-latitude Gondwana environment-stable isotope records from Western Australia. Gondwana Research 24, 125–138.

Miller, A,K, 1936. A new Permian ammonoid fauna from Western Australia. Journal of Paleontology 10, 684–688.

Mory, A.J., 1991. Geology of the offshore Bonaparte Basin, northwestern Australia. Geological Survey of Western Australia Report 29, 47 p.

Mory, A.J., 2010. A review of mid-Carboniferous to Triassic stratigraphy, Canning Basin, Western Australia. Geological Survey of Western Australia Report 107, 1–130.

Mory, A.J., Backhouse, J., 1997. Permian stratigraphy and palynology of the Carnarvon Basin, Western Australia. Geological Survey of Western Australia Report 51, 1–37.

Mory, A.J., Haig, D.W., 2011. Permian-Carboniferous geology of the northern Perth and Southern Carnarvon Basins, Western Australia – a field guide. Geological Survey of Western Australia Record 2011/14, 1–65.

Mory, A.J., Iasky, R.P., 1996. Stratigraphy and structure of the onshore Northern Perth Basin, Western Australia. Geological Survey of Western Australia Report 46, 1–101.

Mory, A.J., Redfern, J., Martin, J.R., 2008. A review of Permian–Carboniferous glacial deposits in Western Australia. Geological Society of America Special Publication 441, 29–40.

Mossadegh, Z.K., Haig, D.W., Allan, T., Adabi, M.H., Sadeghi, A., 2009. Salinity changes during Late Oligocene to Early Miocene Asmari Formation deposition, Zagros Mountains, Iran. Palaeogeography, Palaeoclimatology, Palaeoecology 272, 17–36.

Nicoll, R.S., Metcalfe, I., 1998. Early and Middle Permian conodonts from the Canning and Southern Carnarvon Basin, Western Australia: Their implications for regional biogeography and palaeoclimatology. Proceedings of the Royal Society of Victoria 110, 419–461.

This is an author-produced, peer-reviewed version of this article. The final, definitive version of this document can be found online at *Palaeogeography, Palaeoclimatology, Palaeoecology*, published by Elsevier. Copyright restrictions may apply. doi: 10.1016/j.palaeo.2014.05.009

Palmieri, V., 1993. Foraminifers. Geological Survey of Western Australia Bulletin 136, 30–32.

Playford, P.E., Cope, R.N., Cockbain, A.E., Low, G.H., Lowry, D.C., 1975. Phanerozoic. Geological Survey of Western Australia Memoir 2, 223–433.

Playford, P.E., Cockbain, A.E., Low, G.H., 1976. Geology of the Perth Basin Western Australia. Geological Survey of Western Australia Bulletin 124, 1–311.

Redfern, J., Millward, E., 1994. A review of the sedimentology and stratigaphy of the Permo-Carboniferous Grant Group, Canning Basin, Western Australia. In: Purcell, P.G., Purcell, R.R. (Eds.), The Sedimentary Basins of Western Australia: Proceedings of Petroleum Exploration Society Australia Symposium, Perth, 1994, 753–756.

Reeckmann, S.A., Mebberson, A.J., 1984. Igneous intrusions in the north-west Canning Basin and their impact on oil exploration. In: Purcell, P.G. (Ed.), The Canning Basin, WA: Proceedings of the Geological Society of Australia and Petroleum Exploration Society Australia Symposium, Perth, 1984, 389–399.

Reid, C.M., 2010. Environmental controls on the distributions of late Paleozoic bryozoan colony morphotypes: an example from the Permian of Tasmania, Australia. Palaios 25, 692–702.

Reid, C.M., James, N.P., 2010. Permian higher latitude bryozoan biogeography. Palaeogeography, Palaeoclimatology, Palaeoecology 298, 31–41.

Riding, R., Barkham, S., 1999. Temperate water *Shamovella* from the Lower Permian of West Timor, Indonesia. Alcheringa 23, 21–29.

Roberts, J., Claoué-Long, J.C., Foster, C.B., 1996. SHRIMP zircon dating of the Permian System of eastern Australia. Australian Journal of Earth Sciences 43, 401–421.

This is an author-produced, peer-reviewed version of this article. The final, definitive version of this document can be found online at *Palaeogeography, Palaeoclimatology, Palaeoecology*, published by Elsevier. Copyright restrictions may apply. doi: 10.1016/j.palaeo.2014.05.009

Rogala, B., James, N.P., Reid, C., 2007. Deposition of polar carbonates during interglacial highstands on an Early Permian shelf, Tasmania. Journal of Sedimentary Research 77, 587–606.

Schubert, R., 1915. Die Foraminiferen des jüngeren Paläozoikums von Timor. Paläontologie von Timor, Lieferung 2, 49–59.

Semeniuk, T.A., 2000. Spatial heterogeneity varying to homogeneity in epiphytic foraminifera from micro- to regional scale. Journal of Foraminiferal Research 30, 99–109.

Semeniuk, T.A., 2001. Epiphytic foraminifera along a climatic gradient, Western Australia. Journal of Foraminiferal Research 31, 191–200.

Senowbari-Daryan, B., 2013. *Tubiphytes* Maslov, 1956 and description of similar organisms from Triassic reefs of the Tethys. Facies 59, 75–112.

Shi, G.R., Archbold, N.W., and Zhan, Li-pei, 1995. Distribution and characteristics of mid-Permian (Late Artinskian–Ufimian) mixed/transtional marine faunas in the Asian region and their palaeogeographical implications. Palaeogeography, Palaeoclimatology, Palaeoecology 114, 241–271.

Shi, G.R, Grunt, T.A., 2000. Permian Gondwana–Boreal antitropicality with special reference to brachiopod faunas. Palaeogeography, Palaeoclimatology, Palaeoecology 115, 239–263.

Skwarko, S.K., 1993. Palaeontology of the Permian of Western Australia. Geological Survey of Western Australia Bulletin 136, 1–417.

Stemmerik, L., 1997. Permian (Artinskian–Kazanian) cool-water carbonates in North Greenland, Svalbard and the Western Barents Sea. In: James, N.P. and Clarke, J.A.D. (Eds.), Cool-water carbonates. Society of Economic Paleontologists and Mineralogists, Special Publication 56, 349–364.

Teichert, 1939. Recent research in the Permian of Western Australia: Australian Journal of Science 2, 5–7.

This is an author-produced, peer-reviewed version of this article. The final, definitive version of this document can be found online at *Palaeogeography, Palaeoclimatology, Palaeoecology*, published by Elsevier. Copyright restrictions may apply. doi: 10.1016/j.palaeo.2014.05.009

Teichert, C., 1942. Permian ammonoides from Western Australia. Journal of Paleontology 16, 221–232.

Thompson, M.L., 1949. The Permian fusulinids of Timor. Journal of Paleontology 23, 182–192.

van den Boogaard, M., 1987. Lower Permian conodonts from western Timor (Indonesia). Proceedings, Koninklijke Nederlandse Akademie van Wetenschappen Series B 90, 15–39.

Veevers, J.J., 1988. Morphotectonics of Australia's northwestern margin – a review. In: Purcell, P.G., Purcell, R.R. (Eds.), The North West Shelf, Australia. Proceedings of Petroelum Exploration Society Australia Symposium, Perth, 1988, 19–27.

Veevers, J.J., Wells, A.T., 1961. The geology of the Canning Basin, Western Australia. Bureau of Mineral Resources, Geology and Geophysics, Australia, Bulletin 60, 323 p.

Villeneuve, M., Cornée, J.-J., Harsolumakso, A., Martini, R., Zaninetti, L., 2005. Révision stratigraphique de l'Ile de Timor (Indonésie orientale). Eclogae Geologicae Helvetiae 98, 297–310.

Waterhouse, J.B., Shi, G.R., 2013. Climatic implications from the sequential changes in diversity and biogeographic affinities for brachiopods and bivalves in the Permian of eastern Australia and New Zealand. Gondwana Research 24, 139–147.

Webster, G.D., 1998. Distortion in the stratigraphy and biostratigraphy of Timor, a historical review with an analysis of the crinoid and blastoid faunas. Proceedings of the Royal Society of Victoria 110, 45–72.

Wensink, H., Hartosukohardjo, S., 1990. The palaeomagnetism of Late Permian–Early Triassic and Late Triassic deposits on Timor: an Australian origin? Geophysical Journal International 101, 315–328.

Wopfner, H., 1999. The Early Permian deglaciation event between East Africa and northwestern Australia. Journal of African Earth Sciences 29, 77–90.

This is an author-produced, peer-reviewed version of this article. The final, definitive version of this document can be found online at *Palaeogeography, Palaeoclimatology, Palaeoecology*, published by Elsevier. Copyright restrictions may apply. doi: 10.1016/j.palaeo.2014.05.009

Figure Captions

Fig. 1. Map of the western part of present-day Australian continent showing relevant sedimentary basins, extent of known late Sakmarian–early Artinskian marine deposition, and study sites (labelled 1 to 8); and a schematic reconstruction of north-eastern Gondwana during the Early Permian (modified from Harrowfield et al., 2005).

Fig. 2. Correlation chart showing Lower Permian units in the northern Perth Basin, Southern Carnarvon Basin, Canning Basin and Timor. Localities are shown on Fig. 1. Studied units are highlighted and correlations are explained in text and Appendix B. FCM, Fossil Cliff Member; CF, Carrandibby Formation; BS, Ballythanna Sandstone; WS, Winnamea Sandstone; JJCM, Jimba Jimba Calcarenite Member; BF, Billidee Formation; NNM, Nura Nura Member.

Fig. 3. SRTM image of Timor (compiled from NASA US Shuttle Radar Topography Mission images) showing the location of the type area of the Maubisse Limestone and the other important Lower Permian sites: 1, Mt Bissori–Mt Aubeon area near Pualaca, Timor-Leste; 2, Kula area, Timor-Leste; 3, Maubisse Limestone type locality (present study), Timor-Leste; 4, Somohole locality, West Timor; 5, Bisnain area, West Timor; 6, Bitauni area, West Timor; 7 Basleo area, West Timor; 8, Kapan area, West Timor; 9, Kekneno area, West Timor. The inset map shows present-day Timor as part of the non-volcanic Outer Banda Arc.

Fig. 4. Type area of Maubisse Limestone. **A**, limestone cliffs (central right of image) designated by Audley-Charles (1968) as type locality for the "Maubisse Formation" (= Maubisse Limestone of present study), as viewed toward southwest from Maubisse Pousada;

This is an author-produced, peer-reviewed version of this article. The final, definitive version of this document can be found online at *Palaeogeography, Palaeoclimatology, Palaeoecology*, published by Elsevier. Copyright restrictions may apply. doi: 10.1016/j.palaeo.2014.05.009

with Mt Ramelau, the highest peak in Timor, in the background. **B**, limestone ridge viewed toward north from the Aitutu–Hato Builico road, showing the position of the measured section selected here as type section of the Maubisse Limestone. **C**, outcrop of type section of the Maubisse Limestone, in the vicinity of Maunlai.

Fig. 5. Google Earth image of type area of Maubisse Limestone showing major high-angle faults and the extent of the formation. Note an apparent decrease in thickness to the west (bedding dips remain constant).

Fig. 6. Stratigraphic log of the type section of the Maubisse Limestone showing the relative abundance of biogenic grain types. The pelmatozoans are mainly crinoids but may include blastoids.

Fig. 7. Examples of *Tubiphytes* from studied sections. Scale bars = 1 mm. **A–C** from Maubisse Limestone type section, Timor-Leste, acetate peels; A, UWA165806; B, UWA165846, note skeletal material (brown) from *Tubiphytes* in interstices of lattice of crinoid plate and compare with Fig. 9A5; C, UWA165826, note infilled bored branching tubes, probably formed by filamentous cyanobacteria, along periphery of specimen. **D, E** from Nura Nura Member, outer Canning Basin, Perindi 1, core 1, acetate peels; D, 875.86 m; E, 875.69 m. **F–J** from Callytharra Formation, Southern Carnarvon Basin; F, thin section, UWA158898; G, thin section, UWA158898; H, acetate peel, UWA165865; I, thin section, UWA127873; J, thin section, UWA127873. See Appendix A (Supplementary Materials) for detailed locality information.

This is an author-produced, peer-reviewed version of this article. The final, definitive version of this document can be found online at *Palaeogeography, Palaeoclimatology, Palaeoecology*, published by Elsevier. Copyright restrictions may apply. doi: 10.1016/j.palaeo.2014.05.009

Fig. 8. Bryozoans from the type section of the Maubisse Limestone, Timor-Leste, viewed in acetate peels. Scale bars = 0.5 mm. **A,** *Streblotrypa minutula* Bassler 1929, UWA165834. **B,** *Fistulipora* sp., UWA165839. **C,** *Dyscritella* (?) sp., UWA165838. **D,** *Dyscritella* (?) sp., UWA165828. **E,** *Streblotrypa minutula* Bassler 1929, UWA165777. **F,** *Sulcoretepora* sp., UWA165842. **G,** *Goniocladia laxa* (?) Bassler 1929, UWA165826. **H,** *Fenestella orientalis* (?) Bassler 1929, UWA165761. **I,** *Penniretipora* sp., UWA165830. **J,** *Dyscritella* (?) sp., UWA165827. **K,** *Spinofenestella* sp., UWA165777. See Appendix A (Supplementary Materials) for detailed locality information.

Fig. 9. Examples of foraminifera from the Orders Miliolida and Fusulinida from studied sections. Classification follows Loeblich and Tappan (1987). Scale bars = 0.1 mm. **A1–A12**, representatives from the Subfamily Calcivertellinae. **A1–A7**, *Calcitornella* morphotypes. A1–A2 from Maubisse Limestone type section, Timor-Leste, acetate peels; A1, UWA165840; A2, UWA165851. A3 from Nura Nura Member, outer Canning Basin, acetate peel, UWA165856, Perindi 1, core 1 at 872.62 m. A4–A7 from Callytharra Formation, Southern Carnarvon Basin; A4, acetate peel, UWA165868; A5, thin section, UWA127902, note foraminiferal skeletal material (dark brown) in interstices of lattice of crinoid plate and compare with Fig. 7B; A6, thin section, UWA127852. A7 from nodular limestone in upper Holmwood Shale, northern Perth Basin, acetate peel, UWA165918. **A8–A12**, *Trepeilopsis* morphotypes. A8 from Nura Nura Member, outer Canning Basin, acetate peel, UWA165856, Perindi 1, core 1 at 876.44 m. A9, A10 from Callytharra Formation, Southern Carnarvon Basin; A9, thin section, UWA165911; A10, thin section, UWA127873. A11, A12 from nodular limestone in upper Holmwood Shale, northern Perth Basin, acetate peels; A11, UWA165921; A12, UWA165922. **B1–B8**, representatives of the Family Hemigordiopsidae. B1–B3 from Nura Nura Member, inner Canning Basin, acetate peels, UWA165855. B4–B6 from Callytharra

This is an author-produced, peer-reviewed version of this article. The final, definitive version of this document can be found online at *Palaeogeography, Palaeoclimatology, Palaeoecology*, published by Elsevier. Copyright restrictions may apply. doi: 10.1016/j.palaeo.2014.05.009

Formation, Southern Carnarvon Basin; B4, acetate peel, UWA165866; B5, B6, thin sections, UWA127900. B7, B8 from nodular limestone in upper Holmwood Shale, northern Perth Basin, acetate peels, UWA165922. **C1, C2**, representatives of the Subfamily Meandrospirinae; from Callytharra Formation, Southern Carnarvon Basin; C1, thin section, UWA158906; C2, thin section, UWA158907. **D1, D2**, representatives of Superfamily Endothyracea. D1 from Maubisse Limestone type section, Timor-Leste, acetate peel, UWA165839. D2 from Nura Nura Member, outer Canning Basin, thin section, UWA165856, Perindi 1, Core 1 at 873.85 m. **E1–E3**, representatives of the Superfamily Tetrataxacea. E1, E2 from Maubisse Limestone type section, Timor-Leste, acetate peels; E1, UWA165832; E2, UWA165846. E3 from Nura Nura Member, outer Canning Basin, thin section, UWA165856, Perindi 1, Core 1 at 875.88 m. **F1, F2, ?F3**, representatives of the Family Lasiodiscidae. F1, F2 from Maubisse Limestone type section, Timor-Leste, acetate peels; F1, UWA165826; F2, UWA165832. F3 from Nura Nura Member, outer Canning Basin, thin section, UWA165856, Perindi 1 core 1 at 872.80 m. **G1–G8**, representatives of the Family Pseudoammodiscidae. G1 from Maubisse Limestone type section, Timor-Leste, acetate peel, UWA165824. G2, G3 from Nura Nura Member, outer Canning Basin, Perindi 1, Core 1; G2, thin section (GSWA) at 875.88 m; G3, acetate peel, UWA165856, at 874.36 m. G4–G8 from Callytharra Formation, Southern Carnarvon Basin; G4, thin section, UWA158906; G5, thin section, UWA158907; G6, acetate peel, UWA165865; G7, thin section, UWA127903; G8, thin section, UWA127878. See Appendix A (Supplementary Materials) for detailed locality information.

Fig. 10. Conodont fragment from Maubisse Limestone, Timor-Leste and outcrop from which it was recovered. **A,** outcrop at 8.85534°S, 125.56025°E, 320 m west along limestone ridge from type section of Maubisse Limestone. The sampled level is marked by arrow. **B, C**, conodont Pa fragment of *Vjalovognathus*; **B**, lateral view; **C**, oral view; SEM images. On oral

This is an author-produced, peer-reviewed version of this article. The final, definitive version of this document can be found online at *Palaeogeography, Palaeoclimatology, Palaeoecology*, published by Elsevier. Copyright restrictions may apply. doi: 10.1016/j.palaeo.2014.05.009

view note discrete denticles with rounded cross-section suggesting that this element belongs with *Vjalovognathus australis* Nicoll and Metcalfe (1998). Bar scale is 0.5 mm.

Fig. 11. Photo of acetate peel of segment from Perindi 1, core 1, showing thin layers of rudstone containing lithoclasts of mainly packstone alternating with layers of wackestone/packstone.

Fig. 12. Stratigraphic log of Perindi 1, core 1, showing relative abundance of biogenic grain types.

Fig. 13. Summary chart of Sakmarian–Artinskian depositional sequences in Southern Carnarvon and northern Perth Basins showing formations, key fossil occurrences, and palaeobathymetric and climatic trends. Numbered items are explained in Appendix B.

Fig. 14. Log of typical high-order depositional cycles (parasequences) within the Callytharra Formation in the upper part of the Dead Man's Gully section (Fig. 16) plus photograph showing outcropping limestone beds at the tops of cycles. Friable siliciclastic rocks that form a major part of the succession are poorly exposed.

Fig. 15. Stratigraphic log of the Callytharra Formation, Lyndon River area, showing relative abundance of biogenic grain types.

Fig. 16. Stratigraphic log of the Callytharra Formation, Dead Man's Gully area, showing relative abundance of biogenic grain types.

This is an author-produced, peer-reviewed version of this article. The final, definitive version of this document can be found online at *Palaeogeography, Palaeoclimatology, Palaeoecology*, published by Elsevier. Copyright restrictions may apply. doi: 10.1016/j.palaeo.2014.05.009

Fig. 17. Stratigraphic log of the Callytharra Formation, Jimba Jimba area, showing relative abundance of biogenic grain types.

Fig. 18. Stratigraphic log of the type section of Callytharra Formation showing relative abundance of biogenic grain types.

Fig. 19. Summary of the distributions of foraminiferal groups belonging to the Orders Miliolida and Fusulinida and of *Tubiphytes* at the upper Sakmarian–lower Artinskian localities studied here within the East Gondwana interior rift system. Associated foraminifera belonging to species with organic-cemented agglutinated siliceous tests and to the Order Lagenida are well known in the Southern Carnarvon and northern Perth Basins (Crespin, 1958; Foster et al., 1985; Palmieri, 1993; Dixon and Haig, 2004), but rare at localities 1–3.

Fig. 20. Discrepancies in timing of cold to warm intervals of the Early Permian recognized in the west Australia basins (see evidence outlined in this study) and eastern Australian basins (Fielding et al., 2008 a,b,c).

This is an author-produced, peer-reviewed version of this article. The final, definitive version of this document can be found online at *Palaeogeography, Palaeoclimatology, Palaeoecology*, published by Elsevier. Copyright restrictions may apply. doi: 10.1016/j.palaeo.2014.05.009

Figure 1

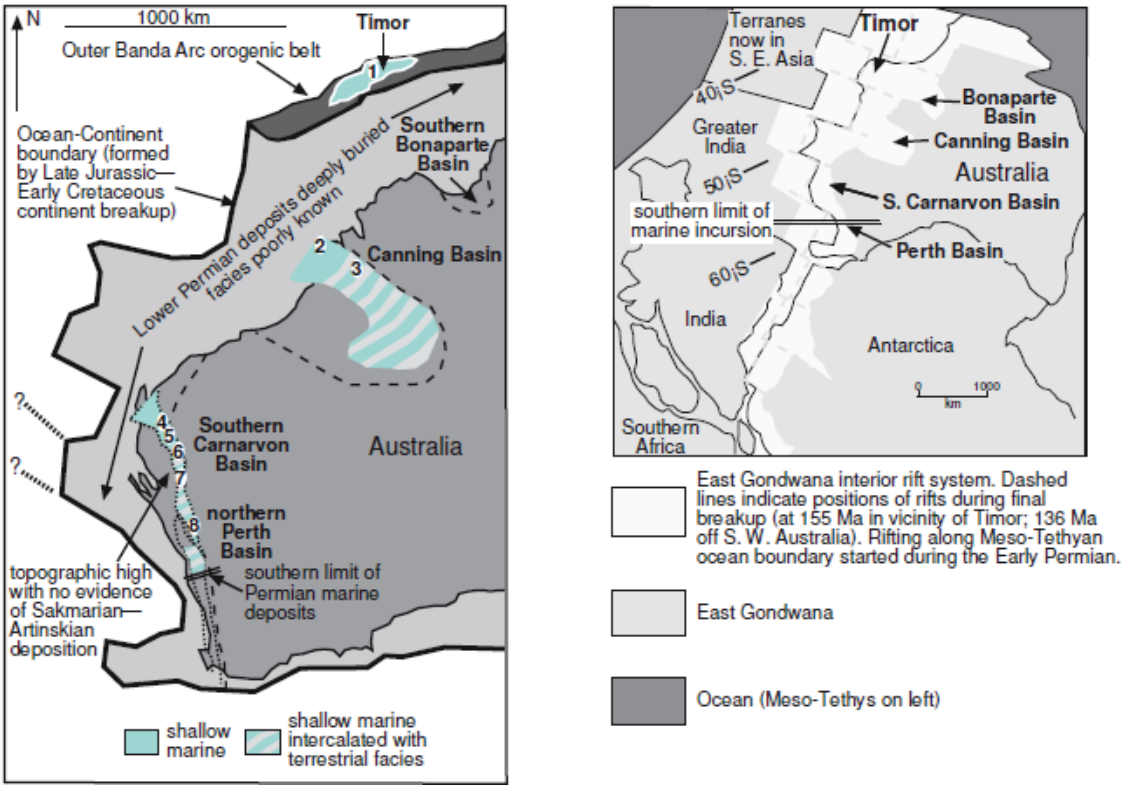

This is an author-produced, peer-reviewed version of this article. The final, definitive version of this document can be found online at *Palaeogeography, Palaeoclimatology, Palaeoecology*, published by Elsevier. Copyright restrictions may apply. doi: 10.1016/j.palaeo.2014.05.009

Figure 2

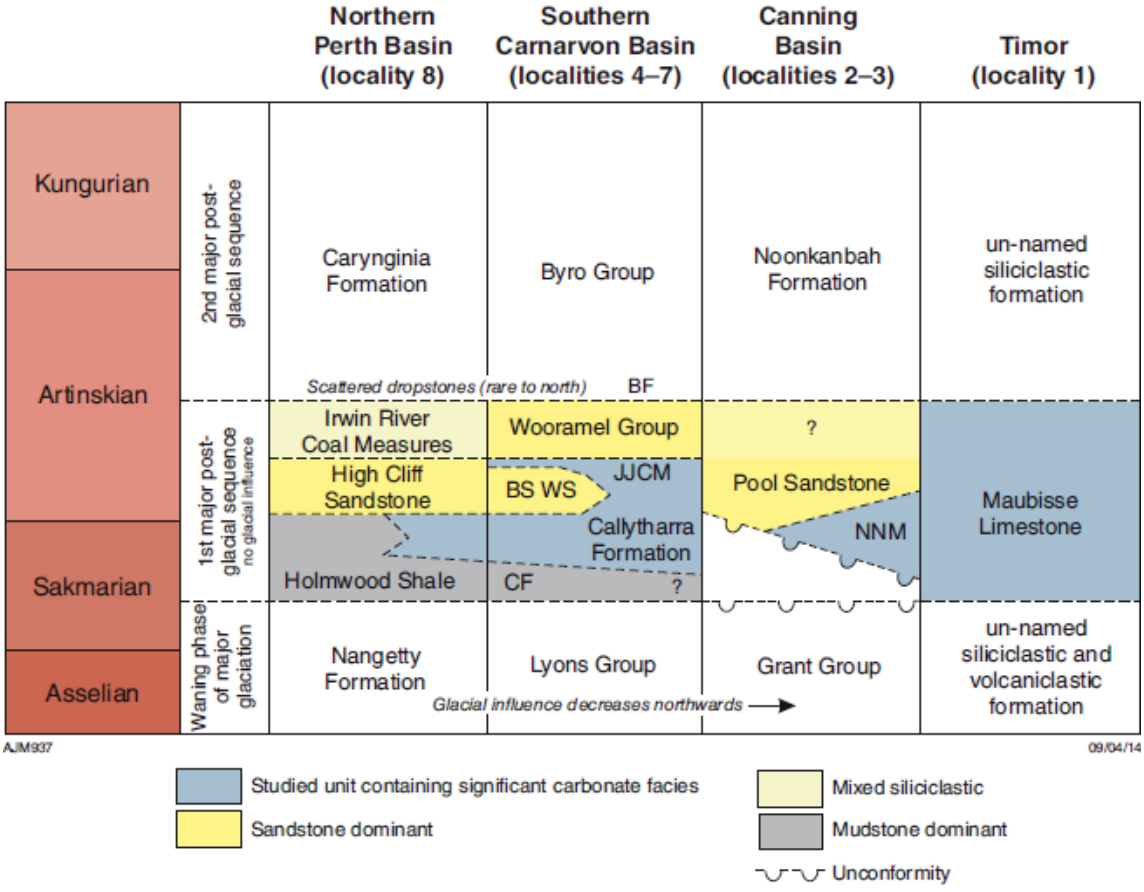

This is an author-produced, peer-reviewed version of this article. The final, definitive version of this document can be found online at *Palaeogeography, Palaeoclimatology, Palaeoecology*, published by Elsevier. Copyright restrictions may apply. doi: 10.1016/j.palaeo.2014.05.009

Figure 3

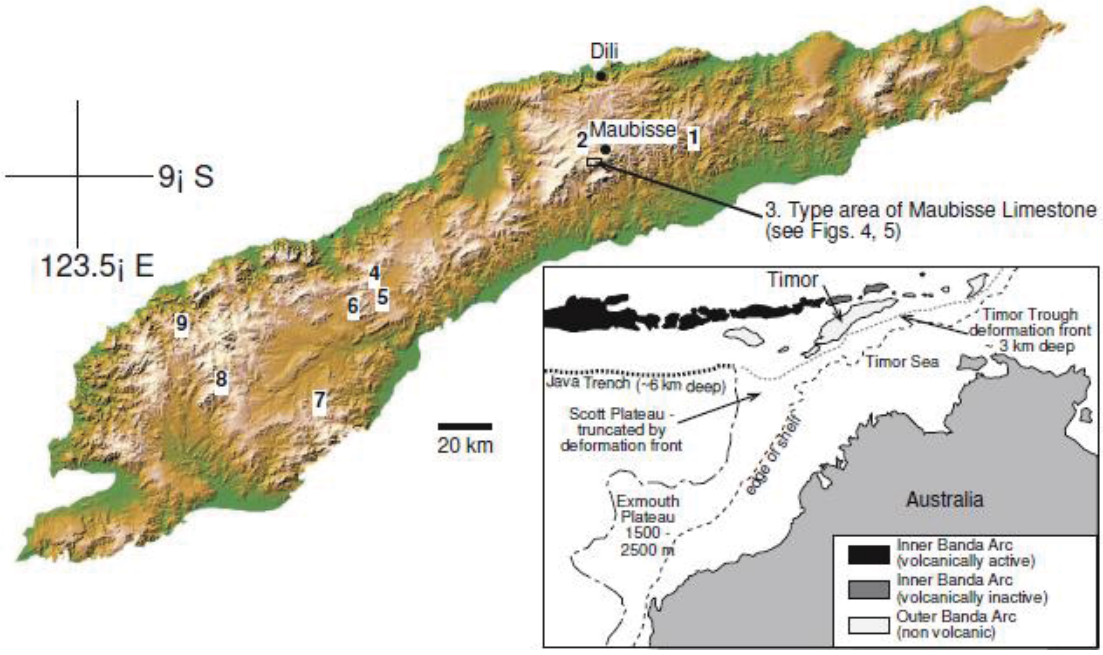

This is an author-produced, peer-reviewed version of this article. The final, definitive version of this document can be found online at *Palaeogeography, Palaeoclimatology, Palaeoecology*, published by Elsevier. Copyright restrictions may apply. doi: 10.1016/j.palaeo.2014.05.009

Figure 4

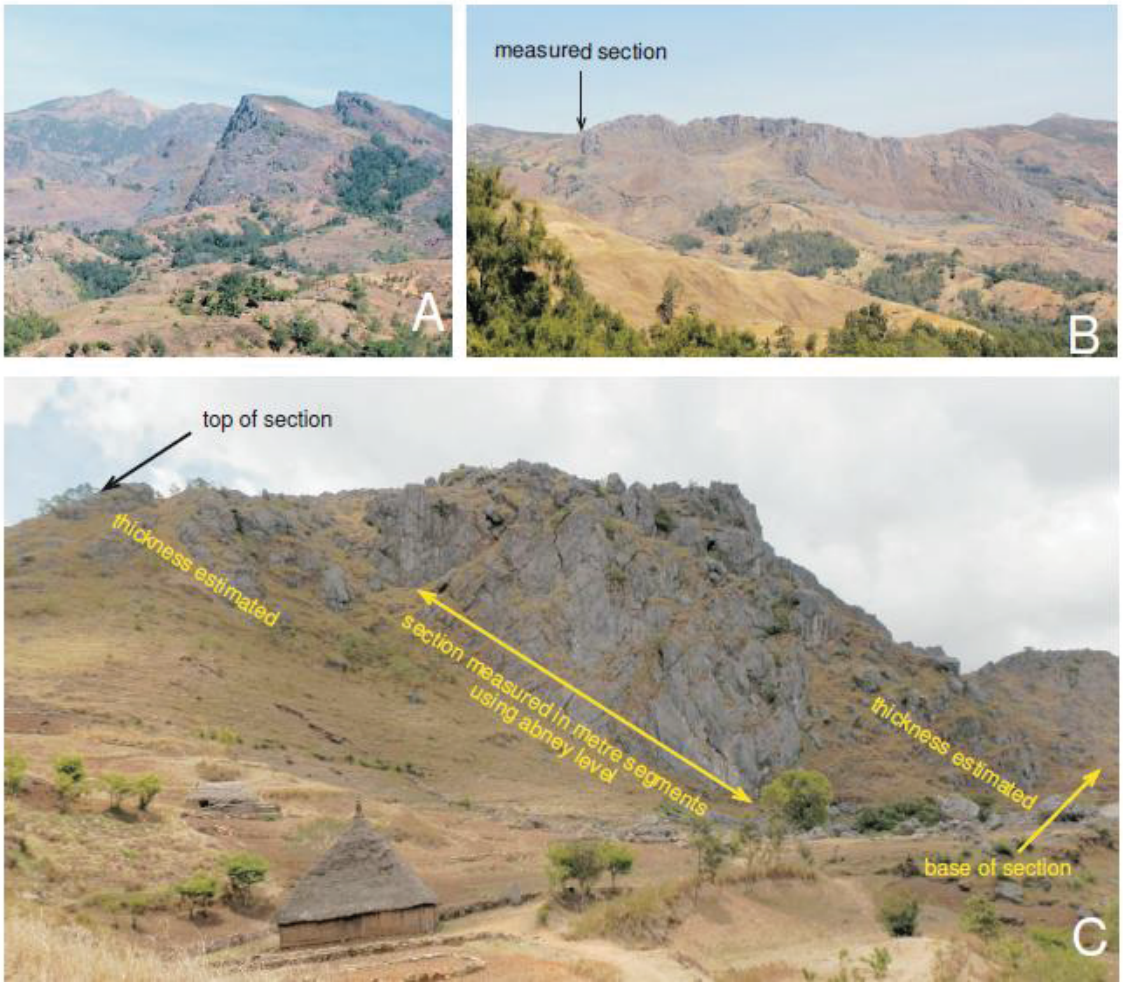

This is an author-produced, peer-reviewed version of this article. The final, definitive version of this document can be found online at *Palaeogeography, Palaeoclimatology, Palaeoecology*, published by Elsevier. Copyright restrictions may apply. doi: 10.1016/j.palaeo.2014.05.009

Figure 5

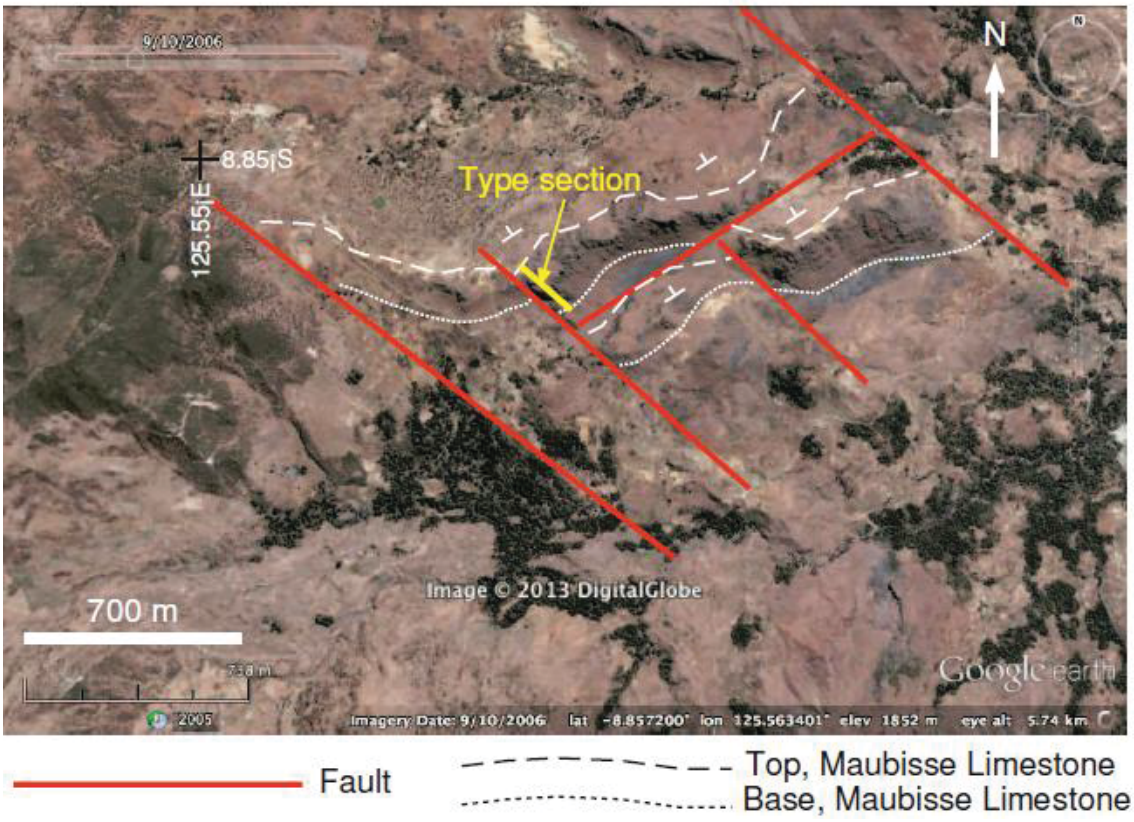

This is an author-produced, peer-reviewed version of this article. The final, definitive version of this document can be found online at *Palaeogeography, Palaeoclimatology, Palaeoecology*, published by Elsevier. Copyright restrictions may apply. doi: 10.1016/j.palaeo.2014.05.009

Figure 6

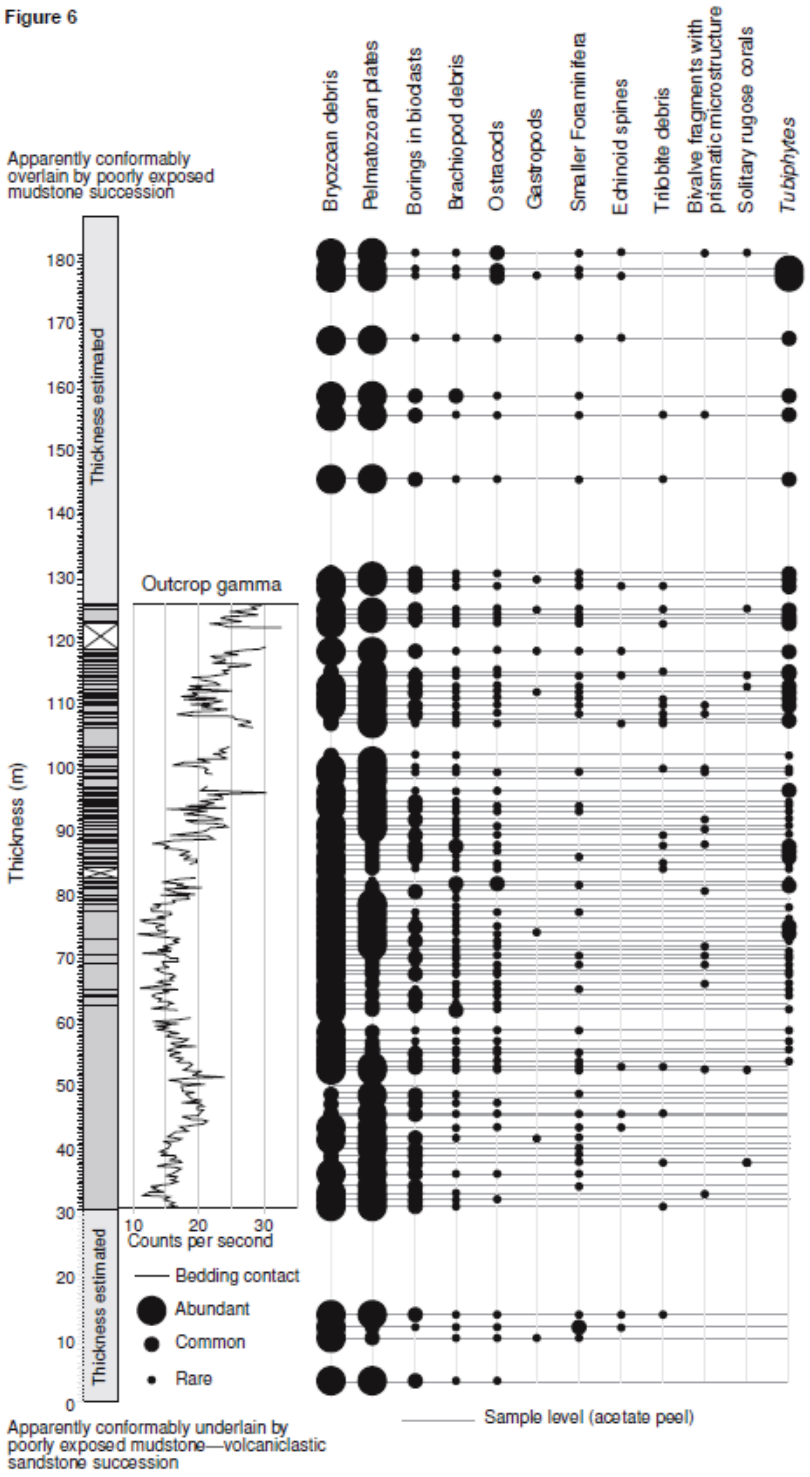

This is an author-produced, peer-reviewed version of this article. The final, definitive version of this document can be found online at *Palaeogeography, Palaeoclimatology, Palaeoecology*, published by Elsevier. Copyright restrictions may apply. doi: 10.1016/j.palaeo.2014.05.009

Figure 7

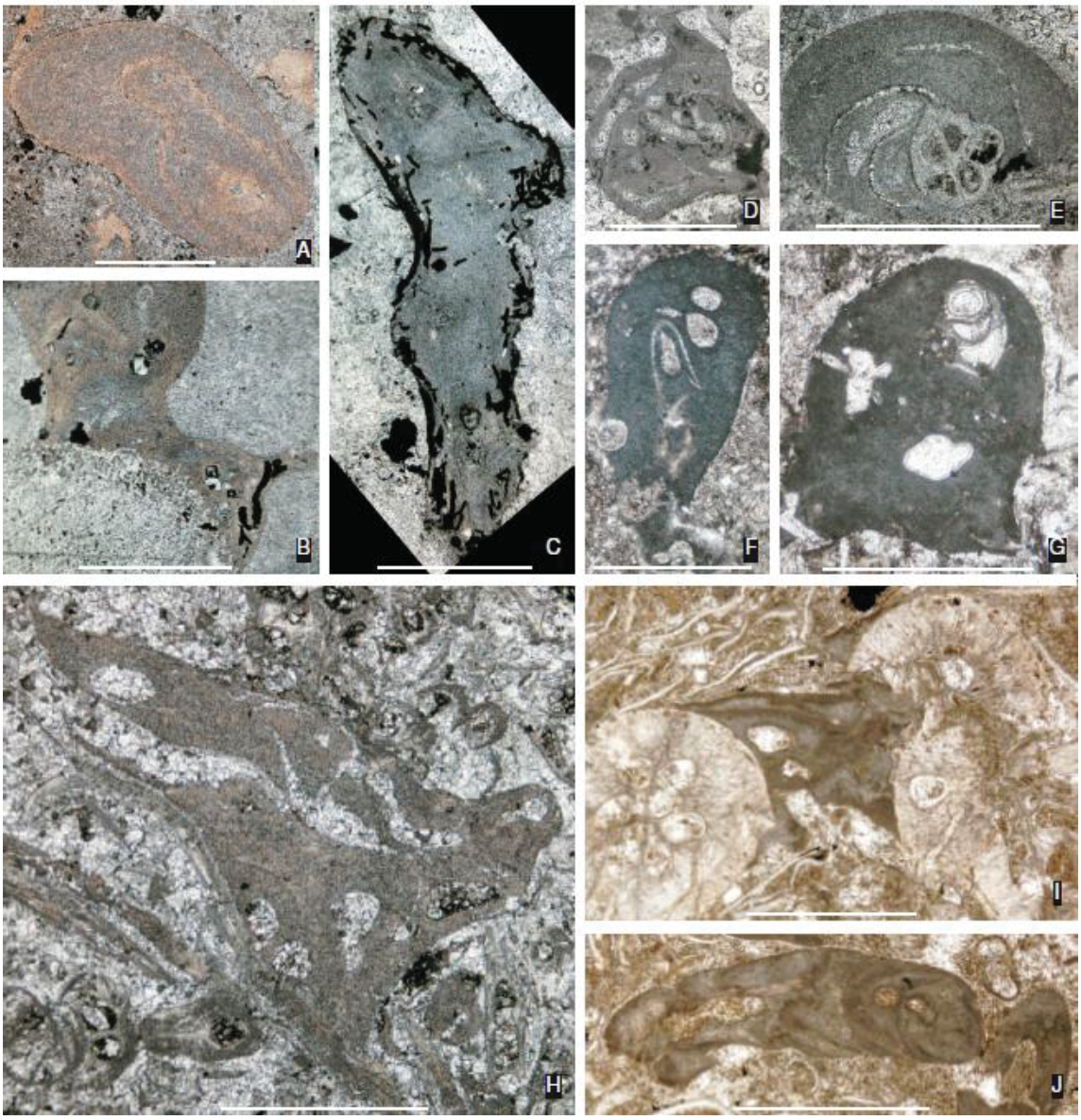

This is an author-produced, peer-reviewed version of this article. The final, definitive version of this document can be found online at *Palaeogeography, Palaeoclimatology, Palaeoecology*, published by Elsevier. Copyright restrictions may apply. doi: 10.1016/j.palaeo.2014.05.009

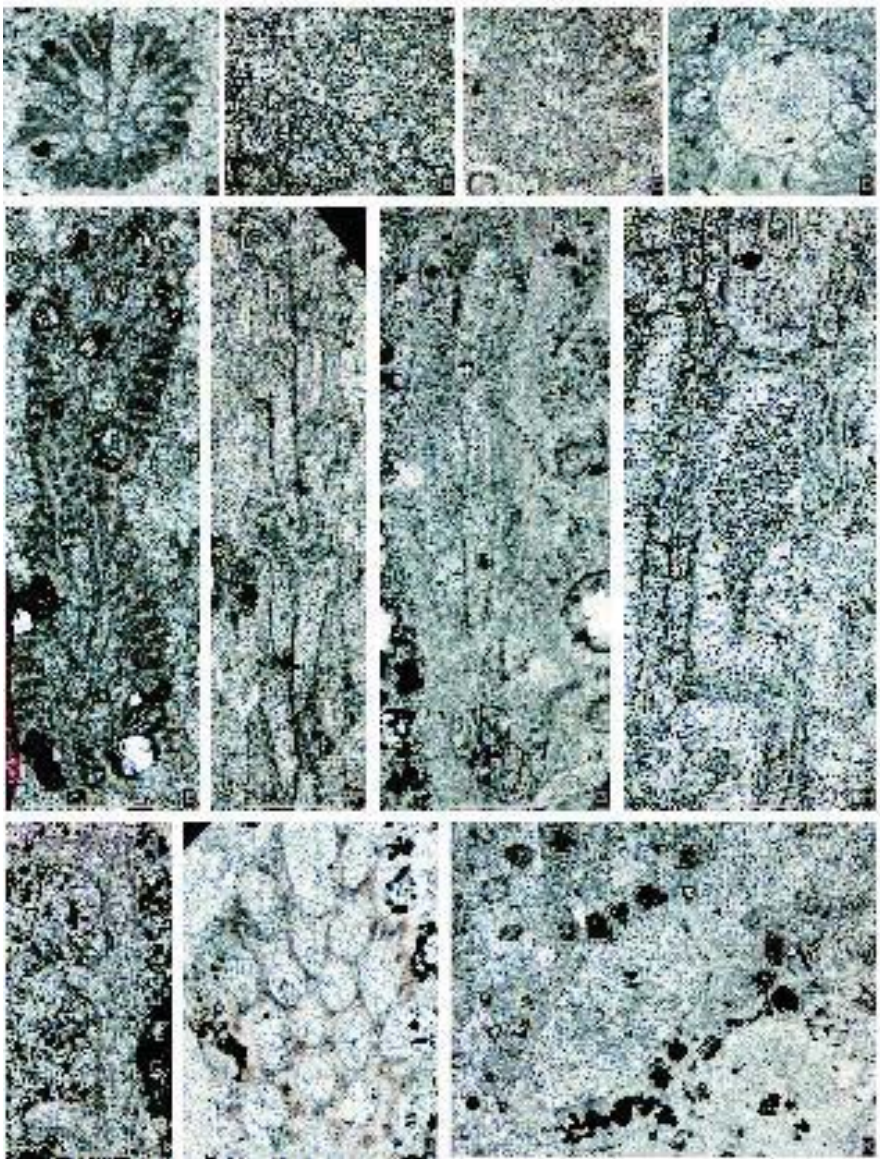

Figure 8

This is an author-produced, peer-reviewed version of this article. The final, definitive version of this document can be found online at *Palaeogeography, Palaeoclimatology, Palaeoecology*, published by Elsevier. Copyright restrictions may apply. doi: 10.1016/j.palaeo.2014.05.009

Figure 9

This is an author-produced, peer-reviewed version of this article. The final, definitive version of this document can be found online at *Palaeogeography, Palaeoclimatology, Palaeoecology*, published by Elsevier. Copyright restrictions may apply. doi: 10.1016/j.palaeo.2014.05.009

Figure 10

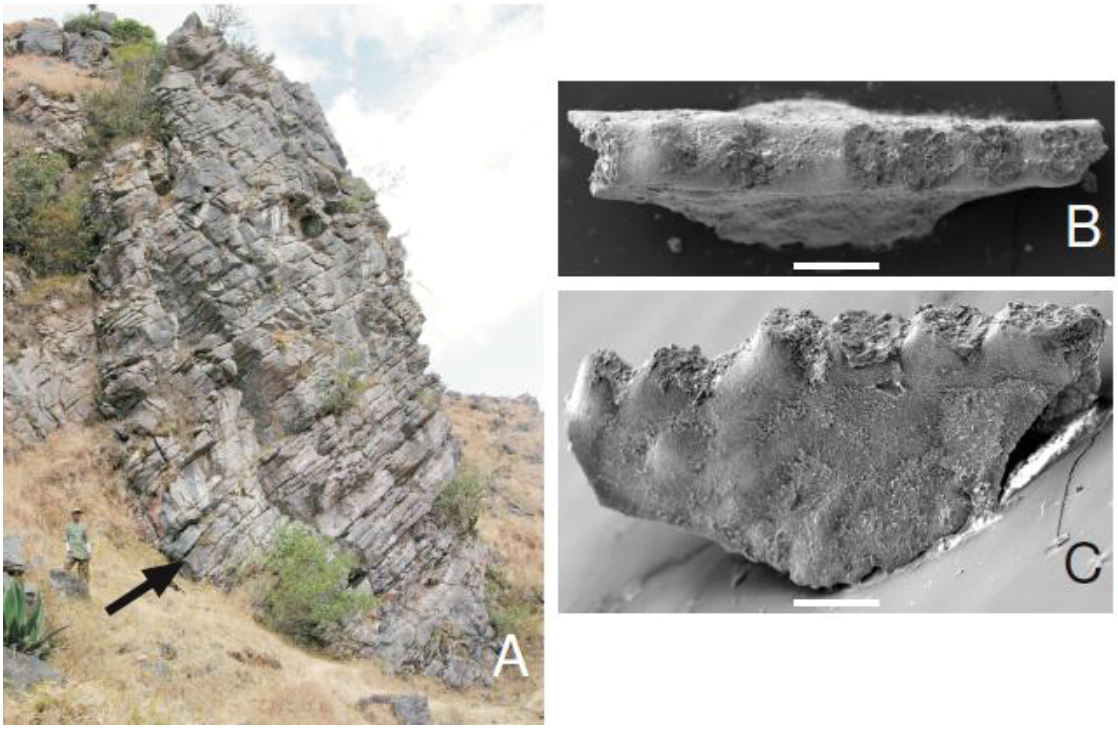

This is an author-produced, peer-reviewed version of this article. The final, definitive version of this document can be found online at *Palaeogeography, Palaeoclimatology, Palaeoecology*, published by Elsevier. Copyright restrictions may apply. doi: 10.1016/j.palaeo.2014.05.009

Figure 11

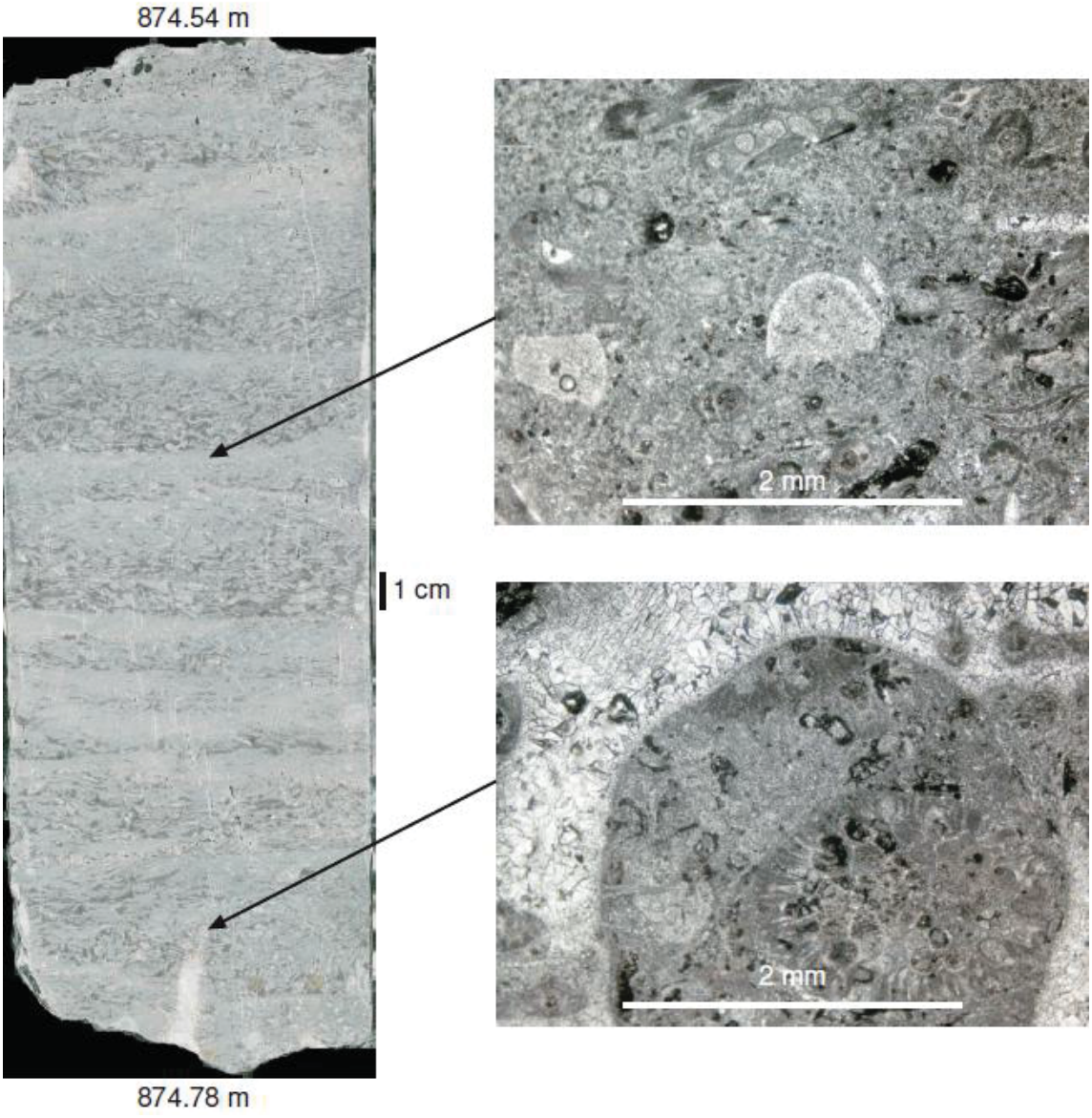

This is an author-produced, peer-reviewed version of this article. The final, definitive version of this document can be found online at *Palaeogeography, Palaeoclimatology, Palaeoecology*, published by Elsevier. Copyright restrictions may apply. doi: 10.1016/j.palaeo.2014.05.009

Figure 12

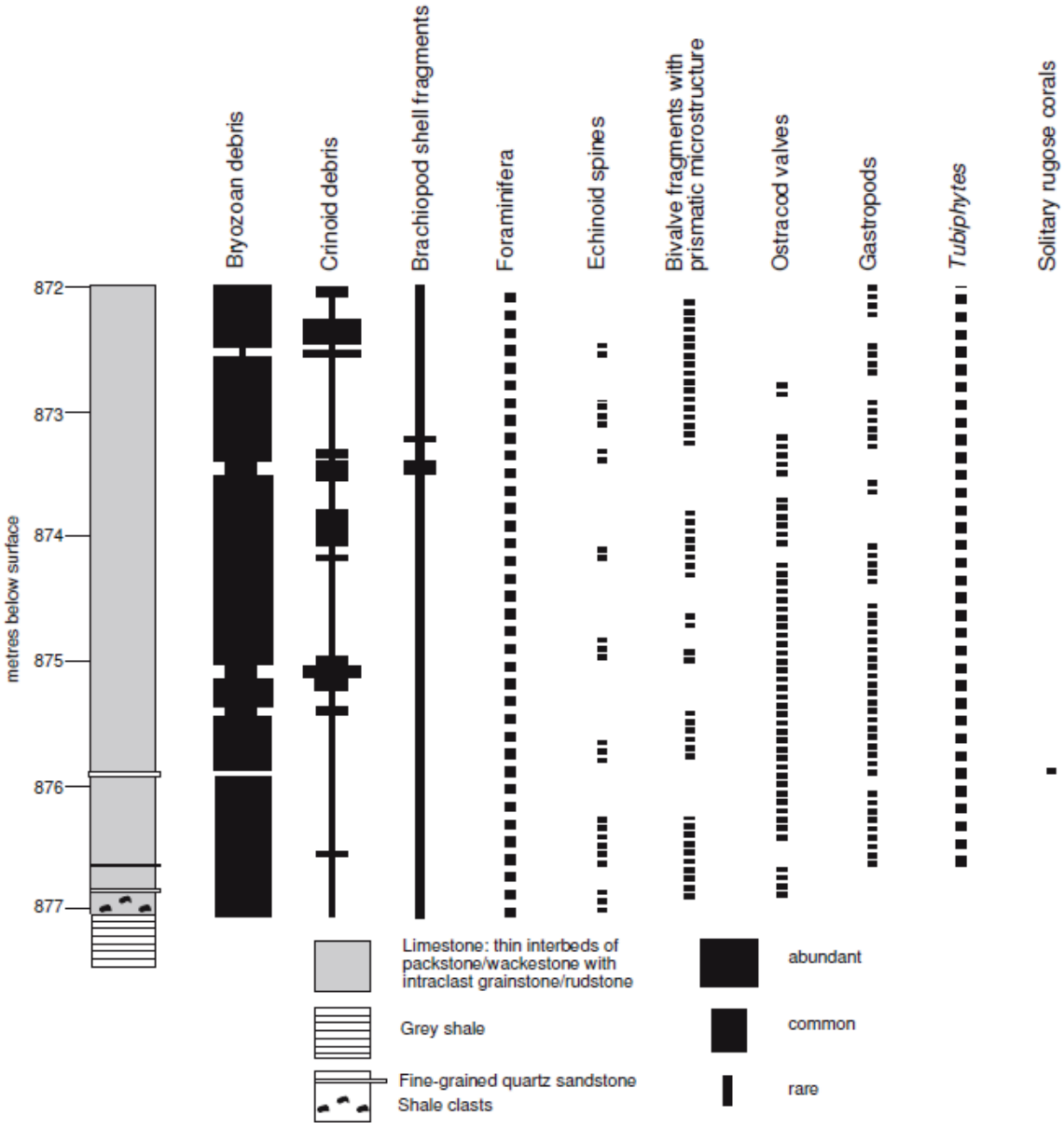

This is an author-produced, peer-reviewed version of this article. The final, definitive version of this document can be found online at *Palaeogeography, Palaeoclimatology, Palaeoecology*, published by Elsevier. Copyright restrictions may apply. doi: 10.1016/j.palaeo.2014.05.009

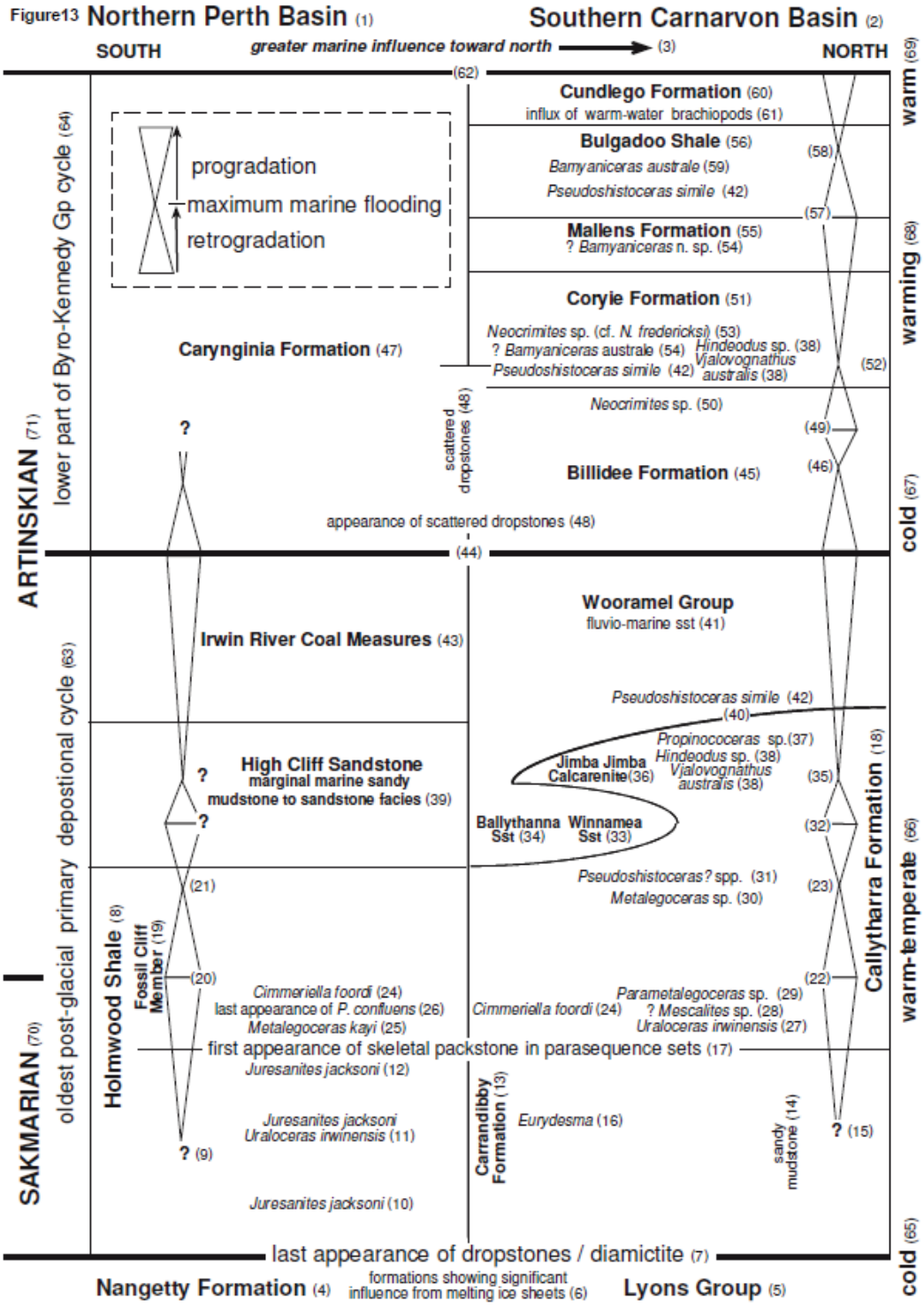

This is an author-produced, peer-reviewed version of this article. The final, definitive version of this document can be found online at *Palaeogeography, Palaeoclimatology, Palaeoecology*, published by Elsevier. Copyright restrictions may apply. doi: 10.1016/j.palaeo.2014.05.009

Figure 14

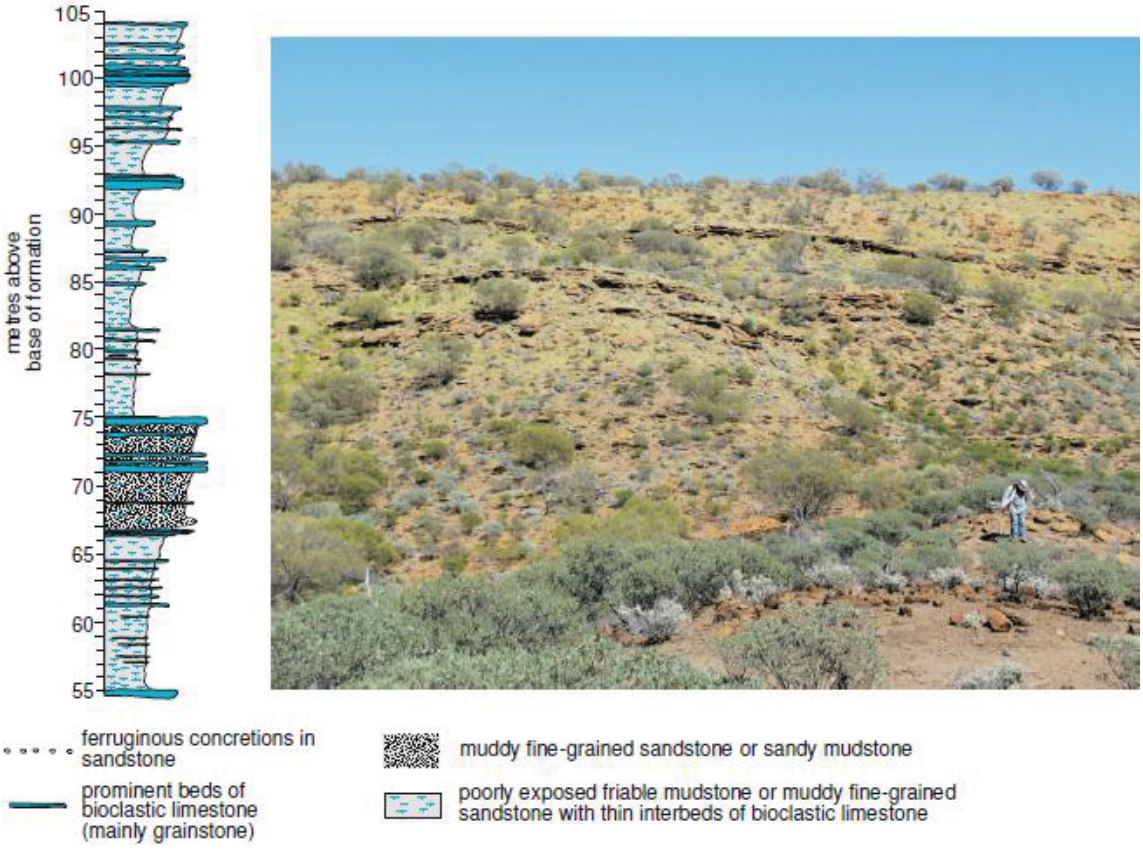

This is an author-produced, peer-reviewed version of this article. The final, definitive version of this document can be found online at *Palaeogeography, Palaeoclimatology, Palaeoecology*, published by Elsevier. Copyright restrictions may apply. doi: 10.1016/j.palaeo.2014.05.009

Figure 15

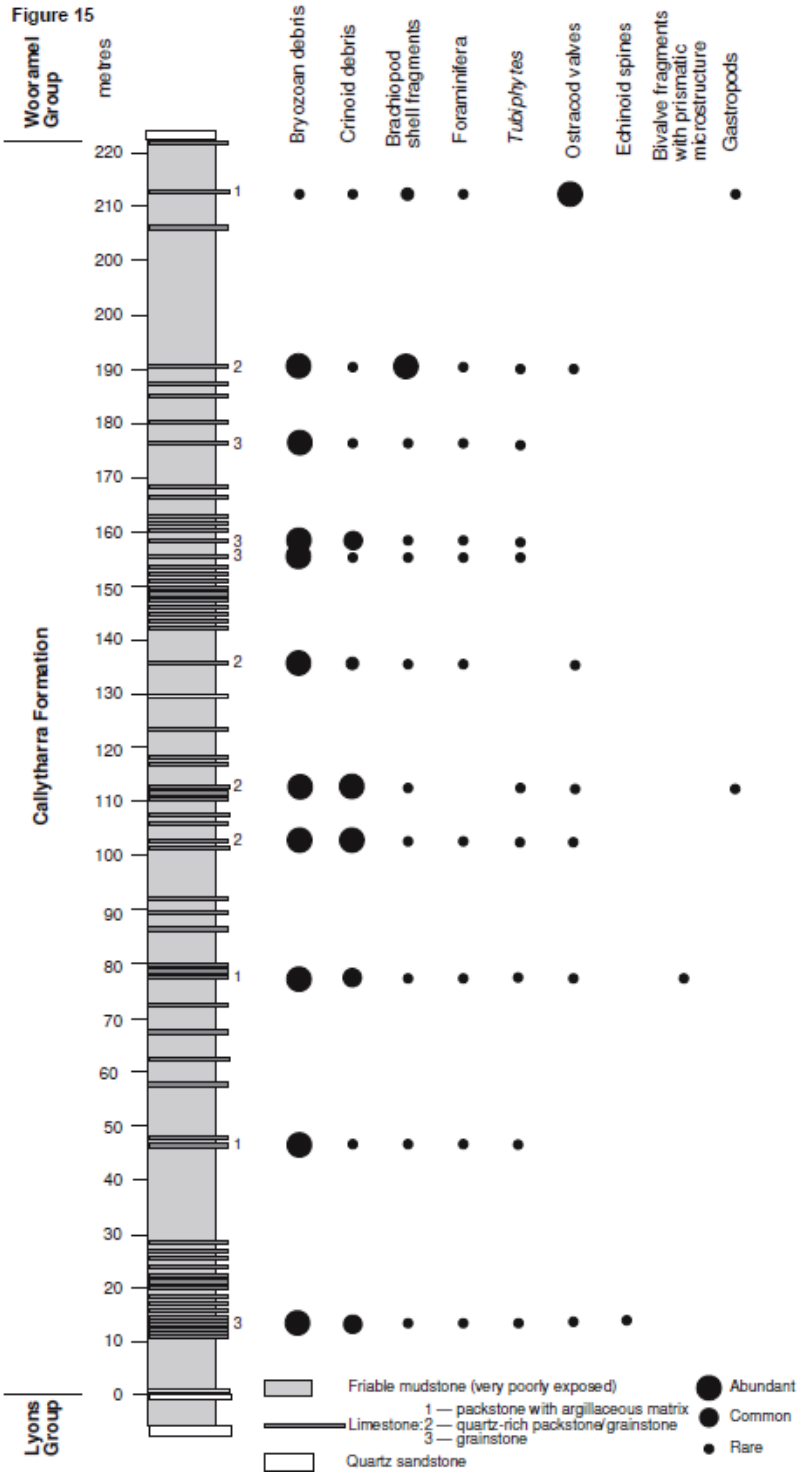

This is an author-produced, peer-reviewed version of this article. The final, definitive version of this document can be found online at *Palaeogeography, Palaeoclimatology, Palaeoecology*, published by Elsevier. Copyright restrictions may apply. doi: 10.1016/j.palaeo.2014.05.009

Figure 16

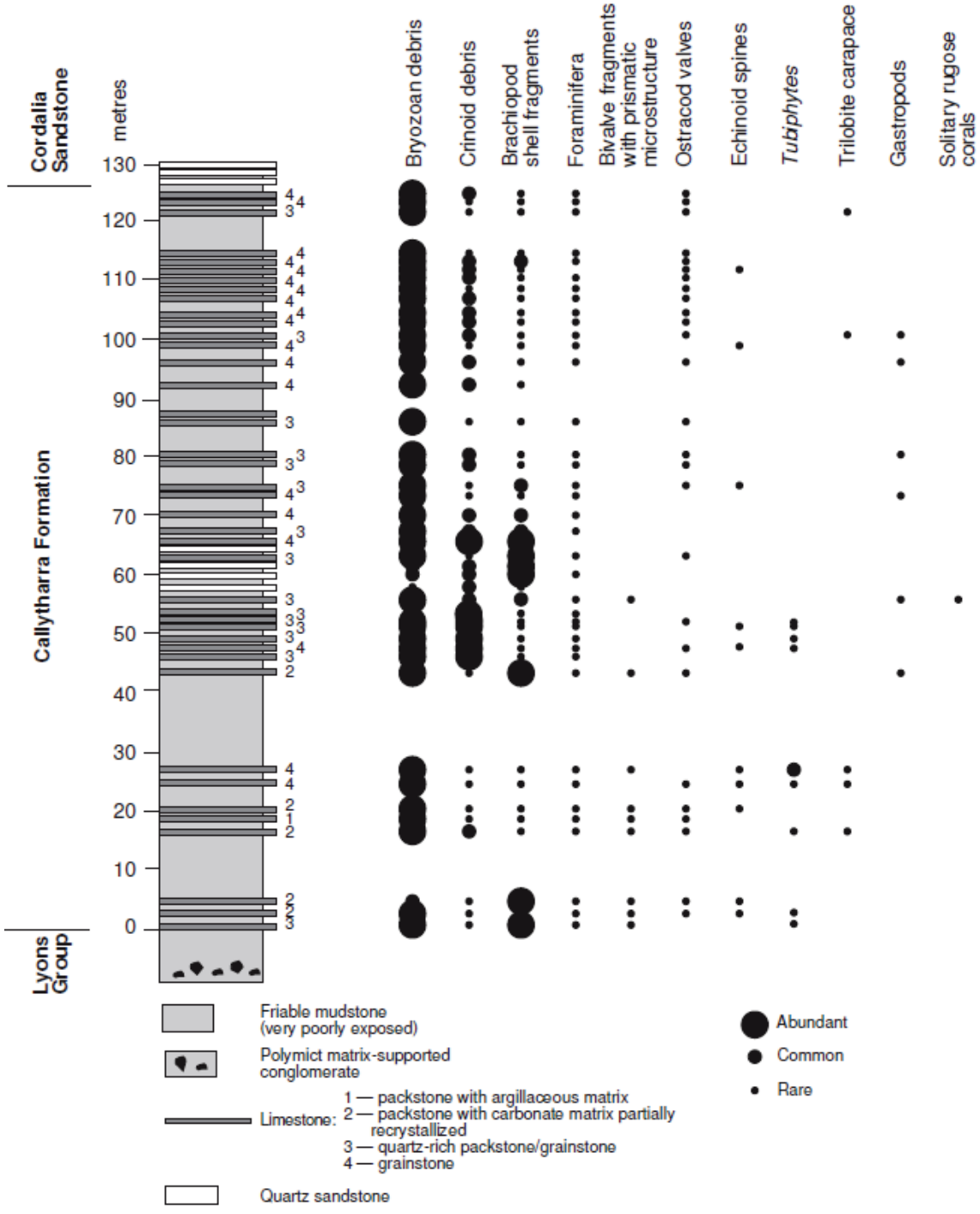

This is an author-produced, peer-reviewed version of this article. The final, definitive version of this document can be found online at *Palaeogeography, Palaeoclimatology, Palaeoecology*, published by Elsevier. Copyright restrictions may apply. doi: 10.1016/j.palaeo.2014.05.009

Figure 17

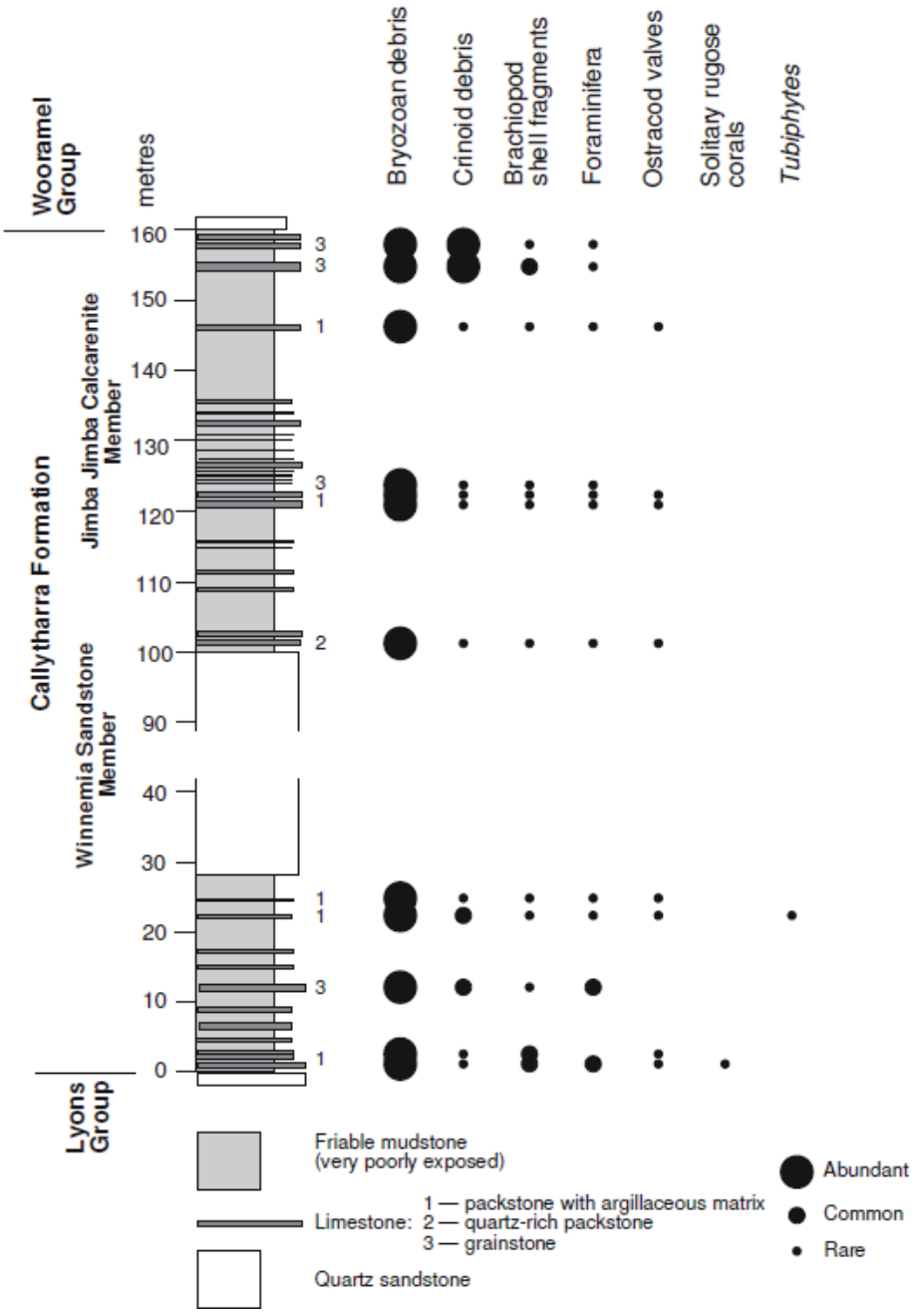

This is an author-produced, peer-reviewed version of this article. The final, definitive version of this document can be found online at *Palaeogeography, Palaeoclimatology, Palaeoecology*, published by Elsevier. Copyright restrictions may apply. doi: 10.1016/j.palaeo.2014.05.009

Figure 18

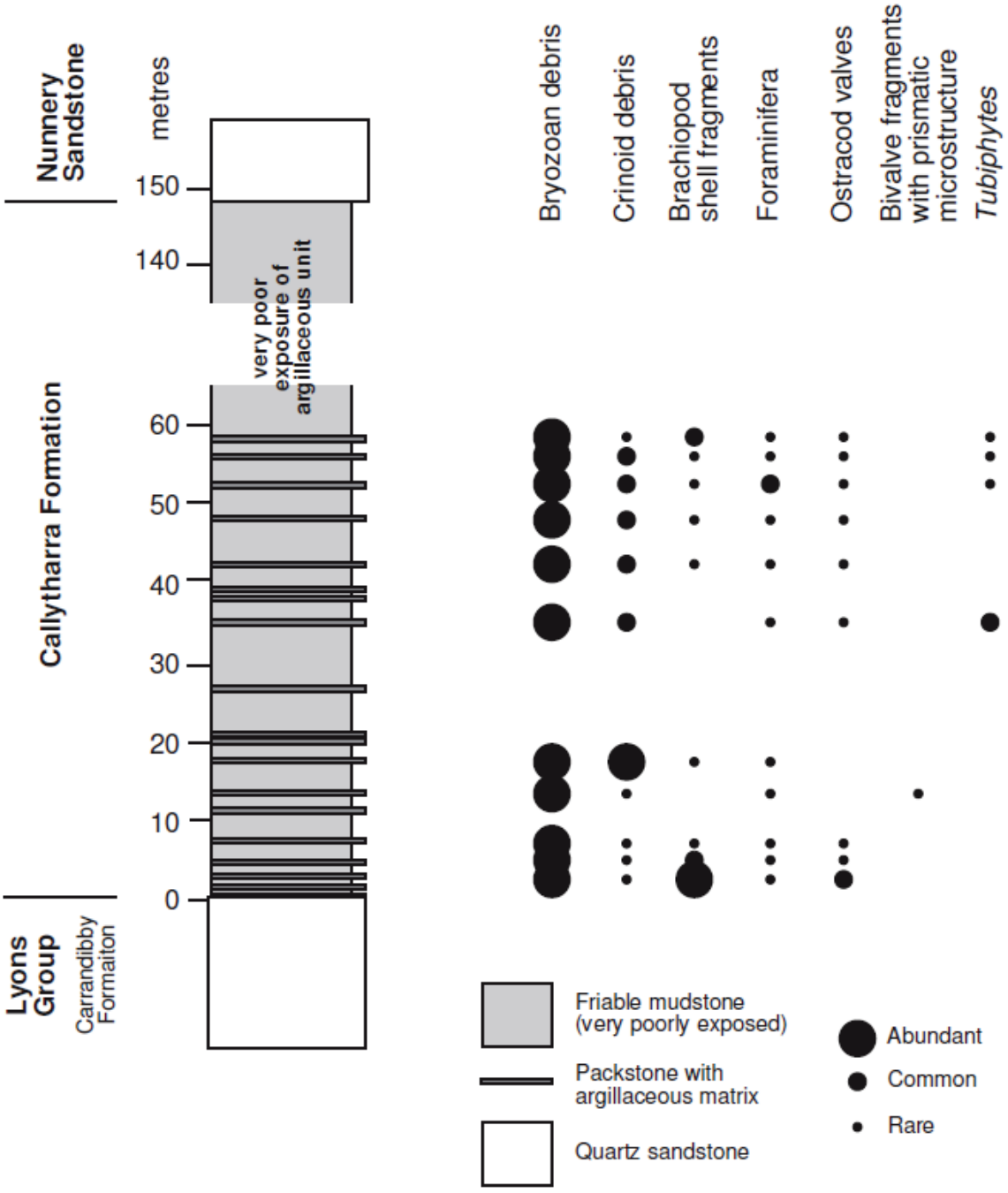

This is an author-produced, peer-reviewed version of this article. The final, definitive version of this document can be found online at *Palaeogeography, Palaeoclimatology, Palaeoecology*, published by Elsevier. Copyright restrictions may apply. doi: 10.1016/j.palaeo.2014.05.009

Figure 19

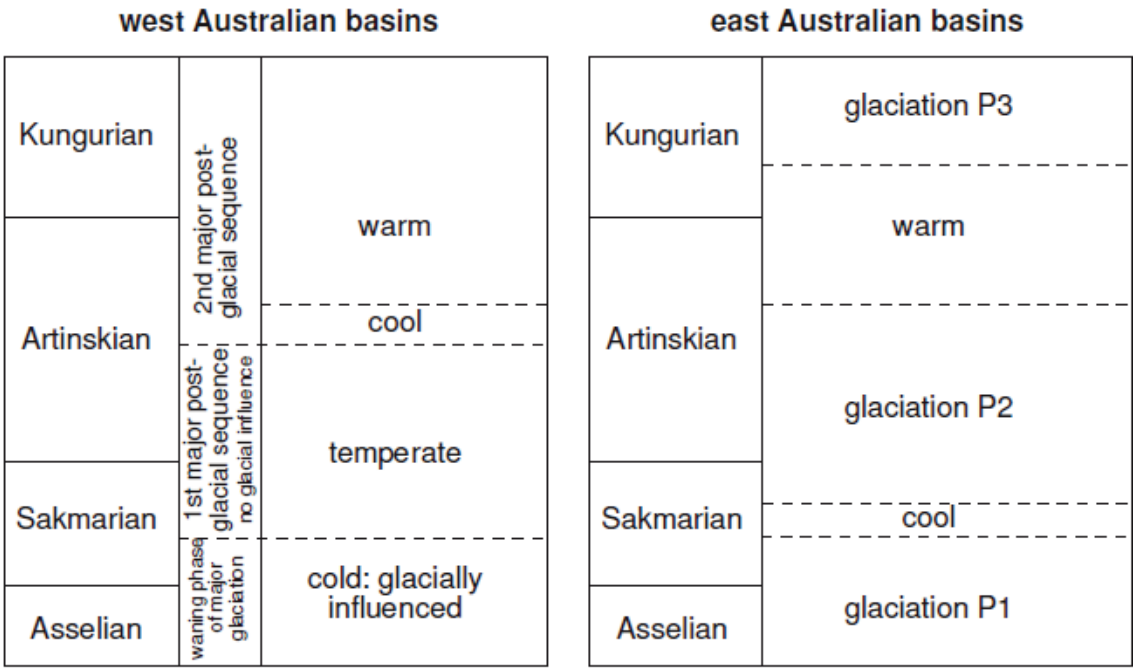

This is an author-produced, peer-reviewed version of this article. The final, definitive version of this document can be found online at *Palaeogeography, Palaeoclimatology, Palaeoecology*, published by Elsevier. Copyright restrictions may apply. doi: 10.1016/j.palaeo.2014.05.009

Figure 20

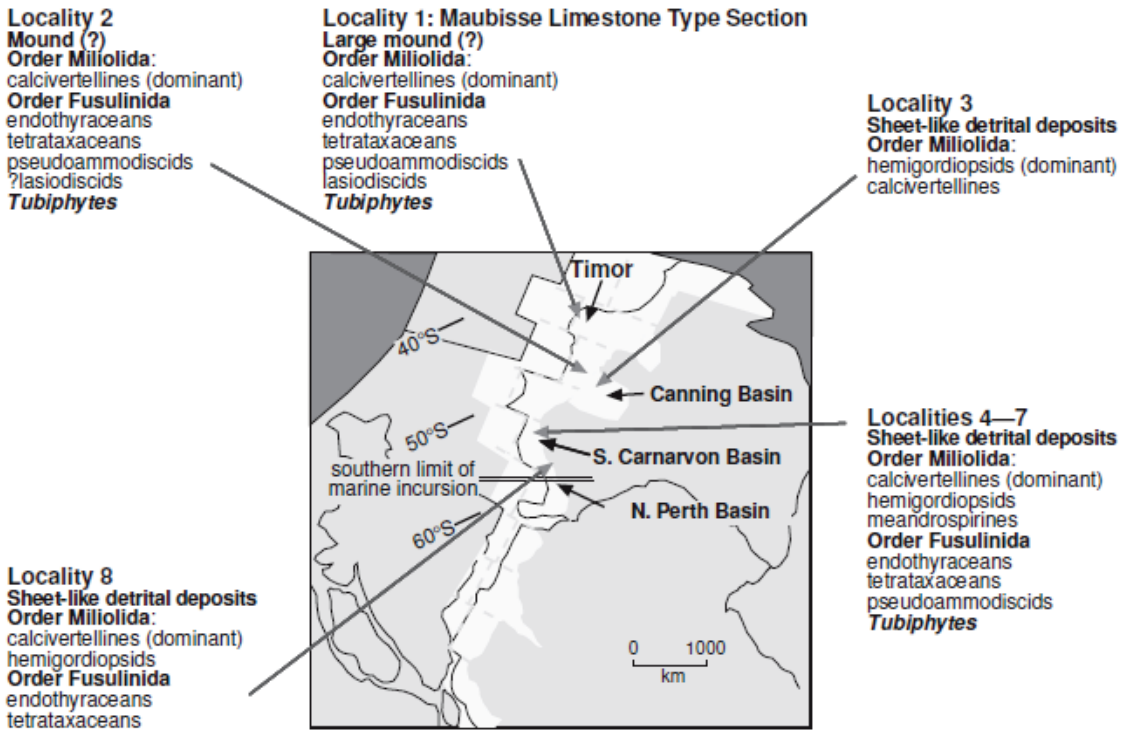

This is an author-produced, peer-reviewed version of this article. The final, definitive version of this document can be found online at *Palaeogeography, Palaeoclimatology, Palaeoecology*, published by Elsevier. Copyright restrictions may apply. doi: 10.1016/j.palaeo.2014.05.009

Highlights

- North to south comparison shows similar dominance of bryozoan-crinoidal debris.
- Tropical biogenic components are absent; *Tubiphytes* is present far south.
- Temperate conditions with very gradual N–S temperature gradient are suggested.
- Discrepancies between west and east Australian successions may be miscorrelation.